



The evolution of carbon oxidation state during secondary organic aerosol formation from individual and mixed organic precursors

Yunqi Shao¹, Aristeidis Voliotis^{1,2}, Mao Du^{1,6}, Yu Wang^{1,5}, Jacqueline Hamilton³, M. Rami Alfarra^{1,2,4}, Gordon McFiggans¹

5

¹School of Earth and Environmental Science, University of Manchester, Manchester, M13, 9PL, UK

²National Centre for Atmospheric Science (NCAS), University of Manchester, Manchester, M13 9PL, UK

³Wolfson Atmospheric Chemistry Laboratories, Department of Chemistry, University of York, York, YO105DD, UK

10 ⁴ Now at Qatar Environment and Energy Research Institute, Hamad Bin Khalifa University, Doha, Qatar

⁵ now at School of Geosciences, University of Edinburgh, Edinburgh, EH9 3FF, UK

⁶ now at School of Geography Earth and Environment Sciences, University of Birmingham, Birmingham B15 2TT, UK

Correspondence to: Yunqi.Shao (Yunqi.Shao@Manchester.ac.uk)

15 Abstract

This study reports the average carbon oxidation state ($\overline{OS_C}$) of secondary organic aerosol (SOA) particles formed from the photo-oxidation of *o*-cresol, α -pinene, isoprene and their mixtures, representative anthropogenic and biogenic precursors, in the Manchester Aerosol Chamber. Three independent mass spectrometric techniques, including two online instruments, high resolution time-of-flight Aerodyne Aerosol Mass Spectrometers (HR-ToF-AMS) and Filter Inlet for Gases and AEROSols coupled to an Iodide high-resolution time of flight chemical ionisation mass spectrometer (FIGAERO-CIMS), and one offline technique, ultra-high-performance liquid chromatography-high resolution mass spectrometry (UHPLC-HRMS), were employed to characterise molar atomic ratios (e.g. O/C, H/C and N/C) leading to estimation of the SOA particle average carbon oxidation state in mixtures of α -pinene/isoprene, *o*-cresol/isoprene, α -pinene/*o*-cresol and α -pinene/*o*-cresol/isoprene. This paper firstly reports the detailed analysis of particle average carbon oxidation state during SOA formation in mixed anthropogenic and biogenic systems using two online and one offline mass spectrometry techniques simultaneously. Single precursor experiments at various initial concentrations were used as a reference. The oxidation state of nitrogen ($\overline{OS_N}$) for CHON compounds was shown to non-negligibly influence the average $\overline{OS_C}$ in individual precursor α -pinene and *o*-cresol experiments in FIGAERO-CIMS and UHPLC-HRMS measurements. By definition, the average $\overline{OS_C}$ accounting for $\overline{OS_N}$, is lower than when the $\overline{OS_N}$ is not considered. SOA particle average oxidation state excluding consideration of $\overline{OS_N}$ obtained by the three techniques showed substantial discrepancies. That obtained from FIGAERO-CIMS was always found to be higher than from the other techniques, as a result of the negligible sensitivity of the FIGAERO-CIMS toward compounds without oxygen. Quantification of the SOA particle average $\overline{OS_C}$ was challenging, but all three techniques showed similar trends across systems. In the single precursor experiments, the initial concentration of precursors influences the average $\overline{OS_C}$ in the single α -pinene experiment, but not in the single *o*-cresol experiment. In binary

20
25
30
35
40



precursor systems, the injected isoprene affected the average \overline{OSc} in the presence of α -pinene but the influence was more modest in the presence of *o*-cresol. The \overline{OSc} in the binary α -pinene/isoprene mixture was lower than in the α -pinene system although they have a similar trend in average \overline{OSc} with SOA mass concentration. This suggests that the isoprene has the potential to decrease the average \overline{OSc} by acting as an OH scavenger, resulting in suppression of the formation of low-volatility and highly oxygenated organic compounds in a mixed system. The \overline{OSc} in the binary α -pinene/ *o*-cresol mixture was between those measured in the single precursor experiments, where that in the α -pinene experiment was lower than in the *o*-cresol experiment, suggesting contributions to the \overline{OSc} from both precursors. In the ternary mixture, the \overline{OSc} was not dominated by any single precursor, with substantial contributions from products uniquely found in the mixture. These results implies that interactions between VOC products should be considered, to enable the level of chemical aging or oxidation of organic compounds understanding in ambient atmosphere.

55



1. Introduction

The formation and evolution of secondary organic aerosol (SOA) from mixtures of volatile organic compounds (VOCs) play an important role to understanding ambient organic aerosol (OA) composition. While early chamber studies predominantly investigated SOA formation from individual precursors (Lee et al., 2011; Winterhalter et al., 2003; Pandis et al., 1991; Hoffmann et al., 1997; Eddingsaas et al., 2012; Kroll et al., 2005a; Ahlberg et al., 2017; Pullinen et al., 2020; Kroll et al., 2005b), more recent research has shifted toward exploring multi-precursor systems, reflecting the chemical complexity of the real atmosphere, where anthropogenic and biogenic VOCs coexist and interact. These interactions can significantly alter SOA yields, volatility distributions, and chemical composition, often through competition for oxidants or formation of cross-products.

For example, Mcfiggans et al. (2019) demonstrated that a reduction of SOA mass and yield with isoprene acting as a scavenger toward OH radicals and its radical's products might contribute to scavenging the highly oxygenated α -pinene products results in increasing the overall volatility of the products from mixture oxidation. In contrast, However, more recent findings by Voliotis et al. (2022a) showed that although the addition of isoprene altered the chemical composition of the SOA and suppressed certain α -pinene-derived products, the overall volatility distribution remained largely unchanged likely due to the formation of new products with comparable volatility distributions. Li et al. (2022) further demonstrated that isoprene can suppress SOA yields from anthropogenic aromatics (e.g., toluene, p-xylene) through OH scavenging, emphasizing the importance of VOC competition. Additionally, Zhao et al. (2025) highlighted mechanistic interactions in mixed biogenic systems, showing that in α -pinene and limonene mixtures, limonene-derived RO₂ radicals and oxidation products facilitated the formation of cross-dimers, enhancing SOA yields. These findings highlighted the importance of the mechanistic interaction between the oxidation products of the precursor in understanding SOA formation in the presence of multiple VOCs.

Despite significant advances, the chemical characterization of SOA from mixed VOC systems remains challenging. OA in the ambient atmosphere comprises thousands of compounds, including hydrocarbons, alcohol, aldehydes and carboxylic acids, with a small fraction (~10-30%) of these



capable of being characterised at a molecular level by current techniques (Hoffmann et al., 2011). Moreover, the chemical complexity of OA increases if there are multiple OA sources (both
90 anthropogenic and biogenic sources) that contribute to OA formation. A current lack of detailed chemical characterisation of these organic species makes it difficult to track the OA sources, understand their atmospheric processes and mitigate their adverse impacts. The majority of ambient SOA is generated by oxidation of VOCs with the dominant prevailing oxidants, hydroxyl radicals (OH), ozone (O₃) and nitrate radicals (NO₃) with their relative contributions varying
95 throughout the day and night, leading to low-volatility products that partition into the particle phase (Atkinson, 2004). As SOA ages, its composition evolves through multi-generational oxidation (Kroll et al., 2005a; Ahlberg et al., 2017; Pullinen et al., 2020)

A useful framework to describe this chemical evolution is the average carbon oxidation state (\overline{OSc}),
100 which increases with the extent of oxidation (Kroll et al. 2011). According to the valence rule, a simplified expression for the average \overline{OSc} of organic mixtures in terms of the molar oxygen to carbon (O/C) and hydrogen to carbon (H/C) ratios is shown in Equation 1.

$$\overline{OSc} = 2 * \frac{O}{C} - \frac{H}{C} \quad (1)$$

105 Changes in carbon oxidation state provide a valuable insight into the oxidation dynamics associated with the formation and evolution of ensemble SOA. For example, the \overline{OSc} generally increases by functionalisation, which can frequently occur in VOC oxidation leading to C-O bonds, for example, replacing C-H or unsaturated C-C bonds. An exception to this is when
110 functionalisation leads to the addition of nitro groups forming a C-N bond, and \overline{OSc} remains the same. In contrast, the average \overline{OSc} remains unchanged by oligomerisation, which may occur after functionalisation and fragmentation reaction (Kroll et al., 2015). On the other hand, change in the average \overline{OSc} of particulate organic molecules is also associated with their volatility, which can strongly influence gas-particle partitioning, resulting in changes in the ensemble chemical
115 composition and increase of OA mass concentration. In general, the overall volatility will decrease with more functionalised molecules and increase with fragmentation (Daumit et al., 2013).



Changes in \overline{OSc} and atomic ratios (H/C and O/C ratios) upon SOA mass loading can therefore be useful tools in identifying the key process in the atmospheric ageing of SOA.

120 In our chamber studies of SOA formation in mixtures of α -pinene, isoprene and *o*-cresol, we have reported the chemical composition of SOA by offline ultra-high-performance liquid chromatography orbitrap mass spectrometry (Voliotis et al., 2022b; Shao et al., 2022a). Oxidation products from the high yield precursor, α -pinene, dominated SOA in its mixtures, whilst isoprene derived compounds made a negligible contribution. Interactions in the oxidation of mixed
125 precursors were found to lead to products uniquely found in the mixtures. In this study, we expand the investigation to report online measurements from the high resolution time-of-flight Aerodyne Aerosol Mass Spectrometers (HR-ToF-AMS) and Filter Inlet for Gases and AEROSols coupled to an Iodide high-resolution time of flight chemical ionisation mass spectrometer (FIGAERO-CIMS; Lee et al. (2014)) to measure the near real-time atomic ratios and derive the oxidation state of SOA
130 during these experiments. The HR-ToF-AMS technique had been widely used for analysing the non-refractory aerosol chemical composition (Aiken et al., 2008; Shilling et al., 2009; Presto et al., 2009; Chhabra et al., 2010; Docherty et al., 2018) and can provide sensitive and online measurements of SOA elemental composition. The FIGAERO-CIMS was used to provide measurements of both gas-phase and particle-phase chemical constituents of organic aerosols in
135 real time. Both instruments have limitations precluding molecular identification (electron impact ionisation in the HR-ToF-AMS leads to extensive fragmentation and the CIMS cannot resolve structural isomers or isobaric compounds (Lee et al., 2014)). Nevertheless, both online instruments can provide the time profile of atomic ratios of the SOA and derived average carbon oxidation state to add interpretation of the evolution of organic compounds to the offline measurement by
140 ultra-high-performance liquid chromatography-high resolution mass spectrometry (UHPLC-HRMS).

The present study aims to investigate the differences in \overline{OSc} in SOA formed from the photooxidation of single precursors and their mixtures. This is achieved by considering

145 i) the chemical mapping of identified SOA in FIGAERO-CIMS measurement and HR-ToF-AMS measurement;



- ii) the relationship between precursors' initial concentration and extent of oxidation in SOA evolution in single precursors experiment,
- iii) the dependence of the atomic ratios (O/C, H/C, and N/C ratios) and the extent of oxidation on
150 SOA particle mass loading in single and mixture precursor systems
- iv) the relative contributions to \overline{OSc} from the oxidation products of each precursor and whether any individual precursor controlled the average \overline{OSc} of SOA in mixed systems.

In order to achieve the objectives, a series of photochemical oxidation experiments were designed
155 and conducted to produce SOA from the selected VOCs (α -pinene, isoprene and *o*-cresol) and their mixtures in the presence of neutral seed particles (ammonium sulphate) and NO_x. The experimental program thereby included three single precursor experiments, three binary precursor mixtures and one ternary mixture of precursors. For studying the effect of the initial VOC concentration on the particle composition and carbon oxidation state of SOA evolution, here we
160 also conduct single precursor experiments at $\frac{1}{2}$ and $\frac{1}{3}$ initial concentration (and hence reactivity towards the dominant oxidant in our experiments, the hydroxyl radical, OH). However, experiments with *o*-cresol at $\frac{1}{3}$ reactivity and isoprene at $\frac{1}{2}$ reactivity are not reported as a result of technical difficulties. The HR-ToF-AMS and FIGAERO-CIMS continuously sampled and measured the SOA particles throughout the experiment and the entire chamber contents were
165 flushed through a filter for collection of the aerosol at the end of the experiment for subsequent offline analysis by UHPLC-HRMS.

170 2. Materials and Methods

2.1. Experimental Procedure

The concept of iso-reactivity towards OH radicals was used to select the initial VOC concentrations in each experiment to enable comparable initial turnover of VOCs in the mixture
175 with respect to OH radicals, such that the oxidation products from each VOCs would make comparable contributions at the chosen concentration and experimental conditions at the beginning of experiment. The injected mass of VOC precursors was calculated based solely on their reactivity with OH radicals (Atkinson, 2004), excluding their consumption by other oxidants (e.g., O₃). Thirteen experimental conditions were planned, covering the α -pinene, isoprene and *o*-cresol



180 single precursor experiments (each at full, $\frac{1}{2}$ and $\frac{1}{3}$ reactivity) respectively, binary α -pinene /
isoprene, α -pinene / *o*-cresol and *o*-cresol / isoprene mixtures and their ternary mixture. Initial
concentrations of each VOC in the binary and ternary mixtures were the same as the initial
concentration in the $\frac{1}{2}$ and $\frac{1}{3}$ reactivity individual VOC experiments respectively, ensuring
comparable initial reactivity toward OH in all systems.

185 As described in Shao et al. (2022b), a “pre-experiment” program and a “post-experiment” were
conducted prior to and after each experiment. These two procedures consist of multiple auto
fill/flush cycle with high flow rate ($\sim 3 \text{ m}^3 \text{ min}^{-1}$) with purified air to condition and remove the
unwanted contaminants in the chamber bag. A water condensation particle counter (WCPC; TSI
190 3786), O_3 analyser, (Thermo Electron Corporation model 49C), NO-NO₂-NO_x analyser (Thermo
Electron Corporation model 42i) were used to monitor residual gas and particles in the chamber
during the “pre-experiment”, to ensure their concentrations were close to zero in the bag prior to
chamber background procedure. The “chamber background” was conducted for approximately 1h,
while collection of data from the chamber in the dark, which the chamber and all instrumentation
195 are all stabilized. An “experimental background” procedure was conducted in the next stage to
establish the baseline contamination level in the chamber. This comprised continuous
measurement after injecting VOC(s), NO_x, and seed particles sequentially and leaving the chamber
to stabilise for an hour under dark condition. All the subsequent analysis presented in this work
has the “chamber background” and “experimental background” subtracted. The baseline of clean
200 background and the experimental background were used to correct experimental data.
Actinometry and off-gassing experiments were performed regularly during our campaign to
monitor the condition and cleanliness of the chamber bag.

The duration of each experiment was nominally 6 hours after initial illumination, under similar
controlled environmental conditions (RH:50±5% and T:24±2 °C). The summary of the initial
205 conditions of the reported experiments were presented in table 1 (noting the lack of $\frac{1}{3}$ reactivity
o-cresol and $\frac{1}{2}$ reactivity isoprene owing to technical difficulties). To enhance confidence in the
validity of our results and to address technical issues caused by occasional instrument failures,
repeat experiments were conducted for selected single-precursor systems (both full and half
reactivity), as well as for the binary and ternary mixture systems. However, this study presents
210 results from only one experiment per system, as previous studies by Voliotis et al. (2021, 2022b)



and Shao et al. (2022a) have already demonstrated good agreement across repeated experiments in terms of maximum SOA mass, volatility distribution, and chemical composition within each system. The particulate products were collected at the end of each experiment, flushing the entire chamber contents through a pre-fired quartz filter (heating in a furnace at 550 °C for 5.5 hours),
215 which was subsequently wrapped in foil and refrigerated at -18 degrees.

Table 1: Summary of the initial conditions of experiments.

Exp. no.	Exp. Type	Precursors Reactivity	VOC	NO _x (ppb)	VOC (ppb)	VOC/NO _x	Seed (µg m ⁻³)
a	Single	Full	<i>α</i> -pinene	40	309	7.7	72.6
b		Half	<i>α</i> -pinene	26	155	6.0	45.7
c		Third	<i>α</i> -pinene	18	103	5.7	51.0
d		Full	<i>o</i> -cresol	44	400	9.1	47.8
e		Half	<i>o</i> -cresol	40	200	5.0	51.3
f		Full	isoprene	23	164	7.1	-
g		Third	isoprene	15	55	3.9	42.2
h	Binary	Full	<i>o</i> -cresol/isoprene	34	282 (200/82)	8.3	49.6
i		Full	<i>α</i> -pinene/ <i>o</i> -cresol	30	355 (155/200)	11.8	57
j		Full	<i>α</i> -pinene/isoprene	39	237 (155/82)	6.1	62.0
k	Ternary	Full	<i>α</i> -pinene/ <i>o</i> -cresol/isoprene	78	291 (103/133/55)	3.7	45.8

220

2.2. Instrumentation

2.2.1. Manchester Aerosol Chamber

225 All experiments were conducted in the Manchester Aerosol Chamber (MAC; Shao et al. (2022b). Briefly, the MAC operates as a batch reactor and consists of 18m³ volume Teflon FEP bag suspended by three rectangular extruded aluminium frames, housed in an air-conditioned enclosure. The enclosure is covered by reflective mylar material and is illuminated with two 6 kW Xenon arc lamps (XBO 6000 W/HSLA OFR, Osram) and a bank of halogen lamps (Solux 50
230 W/4700 K, Solux MR16, USA) with an intensity corresponding to a photolysis rate of NO₂ (j_{NO_2}) around $1.83 \times 10^{-3} \text{ s}^{-1}$ through the entire experimental campaign. Conditioned air was introduced



between the bag and the enclosure to maintain a constant chamber temperature throughout the experiment. Additionally, active water was used to cooling of the mounting bars of the halogen lamps and of the filter in front of the arc lamps to remove the unwanted heat from the lamps.

235 Relative humidity (RH) and temperature (T) are controlled by the humidifier and by the air conditioning that couple with the chamber. RH and T were continuously monitored by the dewpoint hygrometer and several thermocouples and resistance probes during the experiment. Liquid VOCs (α -pinene, isoprene and *o*-cresol; Sigma Aldrich, GC grade $\geq 99.99\%$ purity) were introduced into chamber through injection into a heated glass bulb for vaporization and

240 subsequently flushed into the chamber with purified N₂ (electronic capture device-grade nitrogen stream; purity $\geq 99.998\%$). A custom-made cylinder (10% v/v) containing NO_x was used for NO₂ injection into the MAC in ECD N₂ as carrier gas. A Topaz model ATM 230 aerosol generator were used to produce ammonium sulphate seed particles by atomization from ammonium sulphate solution (Puratonic, 99.999% purity).

245

2.2.2. Online Measurement

The NO-NO₂-NO_x and O₃ analysers were used to measure the NO₂ and O₃ gas concentration throughout the experiments. A semi-continuous gas chromatograph (6850 Agilent) coupled to a

250 mass spectrometer (5975C Agilent; hereafter GC-MS) with a thermal desorption unit (Markes TT-24/7) was employed to monitor the time profile of VOC precursor decay. An Aerodyne high-resolution time-of-flight aerosol mass spectrometer (HR-ToF-AMS, Aerodyne Research Inc., USA) was used to measure organic mass loading and characterize the composition of non-refractory organic particles. The HR-ToF-AMS instrument was calibrated by using monodisperse

255 (350nm) ammonium nitrate and ammonium sulphate particle prior to and after to the experimental program, referring to the standard protocol in Jayne et al. (2000) and Jimenez et al. (2003). The instrument operated in “V mode” during experiments and ran in mass spectra (MS) and particle-time-of-flight (PToF) sub-modes for equal time periods (30s each section). The HR-ToF-AMS data were processed in Igor Pro 7.08 (Wavemetrics.Inc.) using the standard ToF-AMS analysis

260 toolkit (version 1.21) for both unit mass resolution (UMR) and high resolution (HR) analyses. The average ionisation efficiency of nitrate ($IE=9.38 \times 10^8$), the specific relative ionisation efficiencies (RIE) for NH₄⁺ (3.57 ± 0.02) and SO₄²⁻ (1.28 ± 0.01) from calibration, and the default RIE from Alfarra et al. (2004) of all organic compounds (RIE=1.4) were all applied in the UMR and HR



analysis. HR mass spectra was fitted using the method of Decarlo et al. (2006) and analysed using
265 the ToF-AMS analysis software that reported in D. Sueper et al. (2020). The ion fitting process
for high resolution mass spectra in our analysis refers to the supporting information in Hildebrandt
et al. (2011), since this is critical in the determination of the atomic ratio (O/C), and (H/C) of non-
refractory organic material.

270 The operation of the time-of-flight chemical ionisation mass spectrometer with iodide ionisation
coupled with a filter inlet for gases and aerosols (FIGAERO-CIMS ; Lopez-Hilfiker et al. (2014))
was described in Voliotis et al. (2021). Briefly, the particles were sampled for 30 mins to the PTFE
filter (Zefluor, 2.0 μm pore size) at 1 sL min^{-1} , following by 33 mins thermal desorption (15-min
275 cooling down to room temperature) with ultra-high purity N_2 as carrier gas. The instrument was
run in negative-ion mode by producing I^- reagent ion generated using polonium-210 ionisation
source to ionize methyl iodide (CH_3I). The I^- reagent ions enter the ion molecule reaction region
(IMR) with N_2 (ultra-high purity) as carrier gas. An “instrument background” procedure for the
particle phase measurements was conducted in all the experiments for subtraction from the
280 measurements. The FIGAERO-CIMS data were processed by using the Tofware package in Igor
Pro 7.0.8 (version. 3.2.1., Wavemetrics©) (Stark et al., 2015) for peak identification. A data set of
assigned molecular formula of detected compounds were produced, allowing subsequent
determination of the H/C and O/C ratios.

285

2.2.3. Offline Measurement

Ultra-performance liquid chromatography ultra-high resolution mass spectrometry (Dionex 3000,
Orbitrap QExactive, ThermoFisher Scientific) was employed for analysing the filter sampled
290 particulate. A detailed description of the instruments, experimental set-up and data processing
methodology can be found on Shao et al. (2022a) and Pereira et al. (2021). Briefly, the preparation
of sample solution is as follows:

- 1) Filter samples were dissolved in 4 mL of LCMS-grade methanol, left to stand for 2 hours at ambient temperature, and then extracted using sonication (Fisher Scientific FB15051).



- 295 2) 0.22 μm pore size PDVF filter (Fisher Scientific) and BD PlasticPak syringe (Fisher Scientific) were used for filtering the sample solution, followed by adding further 1 ml methanol on the dry filter for the second extraction of samples with the same method.
- 3) The extracted solution was evaporated to dryness using a solvent evaporator (Biotage) under specified temperature (36 °C) and pressure (8 mbar) conditions.
- 300 4) The extract residual was re-dissolved in 1 ml solvent that consists of LCMS optimal grade water and methanol in a ratio of 9:1.

Once the sample solutions were prepared, they were injected into the UHPLC-HRMS 0.3 ml/min with 2 μl volume by autosampler held at 4 °C. The mass spectrometer was mass calibrated using

305 ESI positive and negative ion calibration solutions (Pierce, Thermo Scientific) prior to sample analysis. The sample solution was passed through a reverse-phase C18 column (Accucore, Thermo Fisher Scientific) 100 mm long \times 2.1 mm wide and with 2.6 μm particle size, with temperature held at 40°C. The mobile phase was composed of (A) LCMS optimal grade water (Sigma Aldrich) and (B) methanol (LC-MS Optimal grade, Fisher Scientific) that both contain 0.1% (v/v) formic acid (Sigma Aldrich, 99% purity). The gradient elution started at 90% (A) with a 1-minute post-injection hold, decreased to 10% (A) over 26 minutes, returned to the initial mobile phase at 28

310 minutes, and ended with a 2-minute re-equilibration. In this instrument, electrospray ionisation (ESI, 35 eV) was performed for both positive and negative mode to charge the organic compounds in a range of m/z 80 to m/z 750. High-energy collisional dissociation from tandem mass spectrometry (MS^2) was used to generate ion fragments for subsequent mass analyser detection.

315 Thus, produced product ion spectrum, to inform the compound's structural characterisation and isomer identification. Analysis of extracted solvent (water: methanol = 9:1) and pre-conditioned bank filter was also performed with the same procedure for subtraction from the measurements to ensure exclusion of baseline noise and artefacts from sample preparation.

320 The data was processed by an automated methodology for non-targeted composition of small molecules (Pereira et al. (2021)). This approach guided the peak identification and molecular formula assignment for detected compounds, enabling calculation of the signal weighted $\overline{O/C}$, $\overline{H/C}$ and $\overline{H/C}$ for each system.

325



2.3. Estimation of average carbon oxidation state (\overline{OSc})

For compounds that contain only carbon, hydrogen and oxygen (designated “CHO” compounds), the average \overline{OSc} was straightforwardly determined using atomic ratios O/C and H/C using equation 1, $\overline{OSc} = 2 * O/C - H/C$, in analysis of data from all MS techniques.

For compounds that additionally contain nitrogen (“CHON” compounds), it is assumed that the nitrogen would exist as nitrate with $\overline{OS}_N = +5$ if there are 3 or more oxygen atoms in the molecule and as nitrite with $\overline{OS}_N = +3$ if there are fewer than 3 oxygen atoms. For CHON compounds, the \overline{OSc} is therefore calculated using equation (2) where the H, C, O and N are determined from the FIGAERO-CIMS and UHPLC-HRMS signal.

$$\overline{OSc} = 2 * \frac{O}{C} - \frac{H}{C} - (\overline{OS}_N * \frac{N}{C}) \quad (2)$$

Where N/C corresponding to nitrogen-to-carbon ratios, $\overline{OS}_N = 3$ if $nO < 3$; or $\overline{OS}_N = 5$ if $nO \geq 3$. The signal-weighted average \overline{OSc} determined by equation (2) will be presented in section 3 and referred to as “accounting for \overline{OS}_N ”. The HR-ToF-MS is unable to provide molecular information, but provides total particle ensemble C, H and O from the HR mass defect. However, retrieval of mass defect with sufficient accuracy to attribute the N-containing compounds at the resolution of the instrument is too challenging to be considered robust. The calculated \overline{OSc} from HR-ToF-AMS data uses only C, H and O and uses equation 1 (i.e. implicitly not accounting for organic nitrogen in any CHON compounds present). For comparison with the HR-ToF-AMS -calculated \overline{OSc} , the average \overline{OSc} for CHON compounds measured by the FIGAERO-CIMS and UHPLC-HRMS technique has also been calculated ignoring the N and using equation (1), and this referred to as “not accounting for \overline{OS}_N ”. in section 3

Strictly, the estimation of average carbon oxidation state should account for the oxidation state of sulphur (\overline{OS}_S) in any sulphur-containing compounds (CHOS and CHONS compounds) in the particles. Given the challenges associated with the quantification of S-containing compounds in FIGAERO-CIMS technique (Xu et al., 2016; D'ambro et al., 2019), this study does not consider the contribution of \overline{OS}_S in \overline{OSc} calculation. It was also shown by Du et al. (2021) that the influence of heteroatom S or NS on \overline{OSc} calculation would be negligible as a result of their low fractional abundance the in UHPLC-HRMS measurements (see also Shao et al. 2022).



In this study, the average \overline{OSc} reported from a "representative experiment," where only the compounds found in all replicate experiments can be confidently attributed to this particular system in both UHPLC-HRMS and FIGAERO-CIMS analyses. The HR-ToF-AMS measurements
360 were selected from the same 'representative experiment' as the UHPLC-HRMS and FIGAERO-CIMS analyses.

3. Results

365 3.1. \overline{OSc} of Particles in Single VOC experiment at various reactivity levels

Figure 1 shows the average carbon oxidation state of SOA against SOA mass concentration from the single precursor VOC experiments (α -pinene (panel a and b) and *o*-cresol (panel c and d))
370 conducted at different initial reactivity level. Panels (a) and (c) show the average \overline{OSc} of SOA accounting for $\overline{OS_N}$, and (b) and (d) without accounting for $\overline{OS_N}$ of SOA detected by different MS techniques.

In the single precursor α -pinene experiments, the average \overline{OSc} accounting for $\overline{OS_N}$ as a function
375 of mass loading showed small differences between the three initial concentration experiments in FIGAERO-CIMS data (\overline{OSc} at $\frac{1}{3}$ reactivity decreased from -0.24 to -0.46 across the 6-hour experimental period and was very slightly higher than at $\frac{1}{2}$ reactivity ($\overline{OSc} = -0.31$ to -0.51) and full reactivity ($\overline{OSc} = -0.35$ to -0.57) (Fig. 1a). Comparably, the average \overline{OSc} in the $\frac{1}{3}$ reactivity single precursor α -pinene experiment was -0.45 in negative ionisation mode in UHPLC-HRMS,
380 which is slightly higher than that at $\frac{1}{2}$ reactivity ($\overline{OSc} = -0.61$) and full reactivity ($\overline{OSc} = -0.58$) experiment. In contrast, in positive ionisation mode, the average \overline{OSc} in the $\frac{1}{2}$ reactivity system is comparable to that in the full reactivity system ($\overline{OSc} \approx -0.95$) and is approximately 0.26 higher than \overline{OSc} in the $\frac{1}{3}$ reactivity system (Fig. 1a).

385 Fig. 1b shows the average \overline{OSc} not accounting for $\overline{OS_N}$ against particle mass concentration enabling comparison against the HR-ToF-AMS data in the α -pinene experiments. The average \overline{OSc} derived from HR-ToF-AMS showed significant differences between three initial reactivity experiments. Fig. 1b shows that the HR-ToF-AMS is able to estimate \overline{OSc} at lower total particle



mass during the rapid early growth phase of the experiments compared to the other two techniques,
390 before the first FIGAERO sample is collected. First, it is clear that the total SOA mass
concentration trajectory is markedly different for the various initial α -pinene concentration
(Fig. 1b). Also, the $\frac{1}{2}$ reactivity system has the highest average \overline{OSc} from -0.99 to -0.31 compared
to full reactivity ($\overline{OSc} = -1.68$ to -0.39) and $\frac{1}{3}$ reactivity ($\overline{OSc} = -2.51$ to -0.66) system as function
of SOA mass concentration. The average \overline{OSc} of both full and $\frac{1}{2}$ reactivity systems showed
395 upward trend first, followed by reduction during SOA evolution. The average \overline{OSc} was increasing
continuously until the end of the experiment in $\frac{1}{3}$ reactivity system. The average \overline{OSc} values
derived from FIGAERO-CIMS in Fig. 1b each show higher values than those from the HR-ToF-
AMS. The \overline{OSc} from FIGAERO-CIMS is comparable between full reactivity ($\overline{OSc} = -0.17$ to -
0.40) and $\frac{1}{2}$ reactivity systems ($\overline{OSc} = -0.17$ to -0.32) Both are slightly lower than the $\frac{1}{3}$ reactivity
400 system ($\overline{OSc} = -0.07$ to -0.22), which is opposite to the HR-ToF-AMS trend. The UHPLC-HRMS
derived average \overline{OSc} not accounting for \overline{OS}_N from the $\frac{1}{3}$ reactivity experiment is slightly higher
(-0.34) in negative ionisation mode, and lower (-0.19) in positive ionisation mode than that from
the other two experiments, with the negative ionisation values all comparable to those from the
FIGAERO-CIMS. As must be the case given the presence of nitrogen atom in the spectra, the
405 average \overline{OSc} accounting for \overline{OS}_N is lower value than when not accounting for \overline{OS}_N derived from
both FIGAERO-CIMS and UHPLC-HRMS (Fig. 1a and 1b).

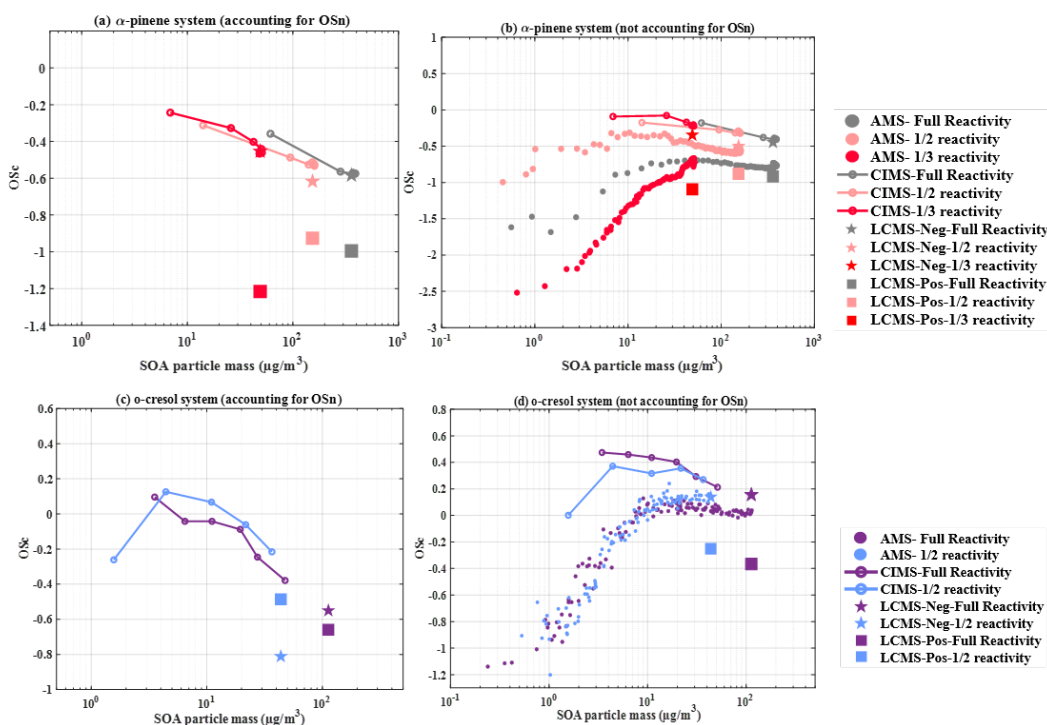
For single precursor *o*-cresol experiments, the FIGAERO-CIMS-derived average \overline{OSc} accounting
for \overline{OS}_N decreased with increasing SOA mass concentration in both the full and $\frac{1}{2}$ reactivity
410 experiments, with the extent of reduction being fairly similar (from 0.12 to -0.26 in the $\frac{1}{2}$ reactivity
experiment and from 0.09 to -0.37 in the full reactivity experiment), as shown in Fig. 1c.
Meanwhile, the full reactivity experiment showed a higher UHPLC-HRMS derived \overline{OSc} (-0.55)
than the $\frac{1}{2}$ reactivity experiment (-0.81) in negative ionisation mode, but with an opposite trend in
positive ionisation mode (Fig. 1c). The difference in average \overline{OSc} when accounting for \overline{OS}_N
415 versus not accounting for it was larger in the half reactivity experiment ($\delta \overline{OSc} = 0.95$) than in the
full reactivity experiment ($\delta \overline{OSc} = 0.70$), suggesting a greater relative contribution of nitrogen-
containing compounds under lower precursor conditions. When not accounting for \overline{OS}_N , the HR-
ToF-MS-derived \overline{OSc} shows a similar increasing trend with SOA particle mass at each initial



concentration, with comparable values ranging from -1.20 to 0.24 as shown in Fig 1d), with the
 420 only difference being that the full reactivity experiment showed slight decrease in \overline{OSc} after SOA
 mass concentration reached its peak at around $10 \mu\text{g m}^{-3}$.

As with the α -pinene experiments, the FIGAERO-CIMS derived average \overline{OSc} were comparable
 between initial concentration *o*-cresol experiments and higher than the HR-ToF-AMS-derived
 \overline{OSc} . The \overline{OSc} reduced with increasing particulate mass concentration from (~ 0.4 to 0). Negative
 425 ionisation mode average \overline{OSc} from UHPLC-HRMS measurements at both initial concentrations
 were comparable at ~ 0.14 (Fig.1d). In positive mode, the average \overline{OSc} at the higher concentration
 was -0.36, 0.11 lower than the lower concentration value.

The SOA particle mass yield (and hence particle mass loading) in the single VOC isoprene
 430 experiment was so close to zero that it was not possible to provide meaningful data on changes in
 composition, as noted in Voliotis et al., (2022a, 2022b).





435 Figure 1: Average carbon oxidation state as function of SOA mass concentration of products detected by the
HR-ToF-AMS, FIGAERO CIMS, and UHPLC-HRMS measurements (Negative Ionization Mode (Neg) and
Positive ionization mode (Pos)) in the single precursor α -pinene and *o*-cresol systems. a) and c) accounting
for $\overline{OS_N}$. b) and d) not accounting for $\overline{OS_N}$.

440 3.2. \overline{OSc} , O/C and H/C ratios of SOA Particles in mixtures accounting for $\overline{OS_N}$

This section compares the average carbon oxidation state and atomic ratios of particles derived
from FIGAERO-CIMS and UHPLC-HRMS data from mixed precursors systems with reference
to their corresponding single precursors experiments. The average carbon oxidation state presented
445 in this section accounts for the nitrogen present in all systems (though not the sulphur) see section
2.4, and excludes HR-ToF-AMS data, owing to the challenges with accounting for $\overline{OS_N}$.

(a) *α -pinene & isoprene binary system*

450 Figure 2 shows the atomic ratios (O/C, H/C and N/C) and average carbon oxidation state \overline{OSc} of
the evolving SOA particles in binary α -pinene/isoprene mixture, individual $\frac{1}{2}$ reactivity α -pinene
and full reactivity isoprene experiments (noting the unavailability of data for lower concentration
isoprene experiments). As might be expected from its very low (near negligible) mass contribution
(below the background chamber concentration ($<1\mu\text{g m}^{-3}$)), whilst the particle produced in the
455 isoprene experiment appear quite highly oxidized in comparison to those from α -pinene, the
isoprene products appear to have a minor effect on the carbon oxidation state and atomic ratios in
binary α -pinene / isoprene system.

Panel a) shows the FIGAERO-CIMS average \overline{OSc} in $\frac{1}{2}$ reactivity α -pinene experiments have a
similar declining trend (from -0.31 to -0.51 through the experiment) as that in the binary mixture
460 (from -0.42 to -0.65), though being slightly more oxidised. As shown in panels b) and c), the
mixture and individual α -pinene experiments showed comparable O/C (~ 0.63 and 0.60) and H/C
ratios (H/C ~ 1.45 to 1.55). The N/C ratios increased as function of SOA mass concentration in
both experiments, with more N in the mixture (N/C increasing from 0.03 to 0.08) than in the
individual α -pinene experiment (N/C = 0.03 to 0.04) (panel d)).

465



The UHPLC-HRMS \overline{OSc} and element atomic ratios (O/C, H/C and N/C) are comparable in negative ionisation modes in the mixture and individual α -pinene experiment (and similar to the FIGAERO-CIMS average \overline{OSc} . \overline{OSc} in the individual α -pinene experiment in positive ionisation mode is slightly (0.1) higher (-0.92) than in the mixture (Fig.2a), reflecting a higher O/C and lower

470 N/C. The values from the last FIGAERO-CIMS measurements are similar to those from the UHPLC-HRMS negative ionisation measurements, both are higher than those from positive ionisation mode.

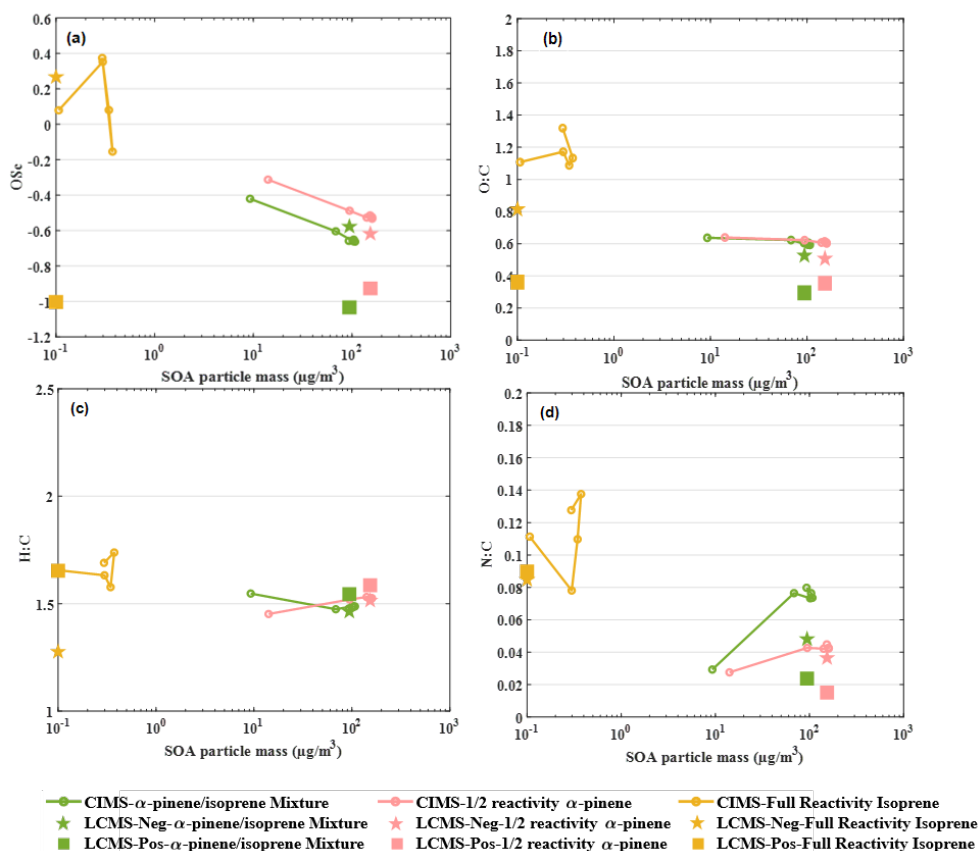


Figure 2: Evolution of SOA particle composition in terms of a) average carbon oxidation state (\overline{OSc}), b) O/C, c) H/C and d) N/C atomic ratios as function of SOA mass concentration from FIGAERO-CIMS and UHPLC-HRMS measurements (-ve Ionization Mode (Neg) and +ve ionization mode (Pos)) in binary α -pinene /isoprene mixture, 1/2 reactivity individual α -pinene and full reactivity individual isoprene experiments.

475



480 **(b) *o*-cresol & isoprene binary system**

Figure 3 shows the \overline{OSc} , O/C, H/C and N/C ratio of SOA particles derived from the FIGAERO-CIMS and UHPLC-HRMS in the binary *o*-cresol / isoprene system, individual $\frac{1}{2}$ reactivity *o*-cresol and full reactivity isoprene experiments respectively. Again, owing to isoprene SOA has
485 minor mass contribution (less than chamber background concentration ($<1 \mu\text{g m}^{-3}$) in the individual experiment, it might be expected that the \overline{OSc} , O/C, H/C and N/C ratio of SOA products from isoprene make a minor contribution in the binary *o*-cresol / isoprene system. Nevertheless, there are some significant differences between the individual VOC and mixture experiments.

The FIGAERO-CIMS \overline{OSc} in the individual *o*-cresol experiment and the mixture system both
490 reduce with increasing particle mass, beyond $3 \mu\text{g m}^{-3}$ (though the compounds in the particles are initially significantly more oxidised in the experiment on the mixture, so \overline{OSc} is initially higher, driven by a high O/C). The FIGAERO-CIMS \overline{OSc} in the mixture decreased from 0.38 at $3 \mu\text{g m}^{-3}$ mass concentration to -0.21, while the \overline{OSc} in the individual *o*-cresol experiment showed a more modest decrease from 0.12 to -0.26 (Fig.3a). The FIGAERO-CIMS O/C and H/C in the mixture
495 are higher than in the individual *o*-cresol experiment (Fig.3b and 3c). In particular the O/C behaved differently between the systems, in the mixture decreasing from 1.72 to 0.76 and in the individual *o*-cresol experiment, slightly increasing from an initial value of around ~ 0.66 to a peak of 0.78 then falling towards the end of the experiment with increasing SOA mass concentration (Fig.3b). The H/C ratios simultaneously showed significantly decrease from 2.24 to 1.24 in the mixture
500 system with a much smaller decrease from 1.32 to 1.09 in the individual *o*-cresol experiment (Fig.3c). It should be noted that this discrepancy in \overline{OSc} between the mixture system and sole *o*-cresol experiment is not seen in the HR-ToF-AMS data, which monotonically increased with SOA mass in the individual VOC and mixture system as shown in Fig. 6 (c), though of course this does not account for any nitrogen in the particles. Figure 3(d) shows that the FIGAERO-CIMS N/C
505 ratio in both experiments increased with mass. This was more pronounced (from 0.02 to 0.12) in the mixture than in the individual *o*-cresol experiment (0.05 to 0.1).

\overline{OSc} and O/C ratio from positive ionisation UHPLC-HRMS in the mixture and individual *o*-cresol experiments were of a comparable magnitude (roughly -0.5 and 0.45 respectively in both systems)



though the H/C ratio is slightly higher in the mixture and N/C slightly lower (Fig.3c and 3d). From
 510 using negative ionisation measurements, Fig.3c and 3d show that the mixture and individual *o*-
 cresol oxidation produces similar H/C and N/C ratios. Particles formed in the individual *o*-cresol
 experiment are marginally less oxidised ($\overline{OSC} = -0.81$), than in the mixture system (-0.70), though
 overall the low degree of oxidation is driven by the high organic N-content of the particles.

515

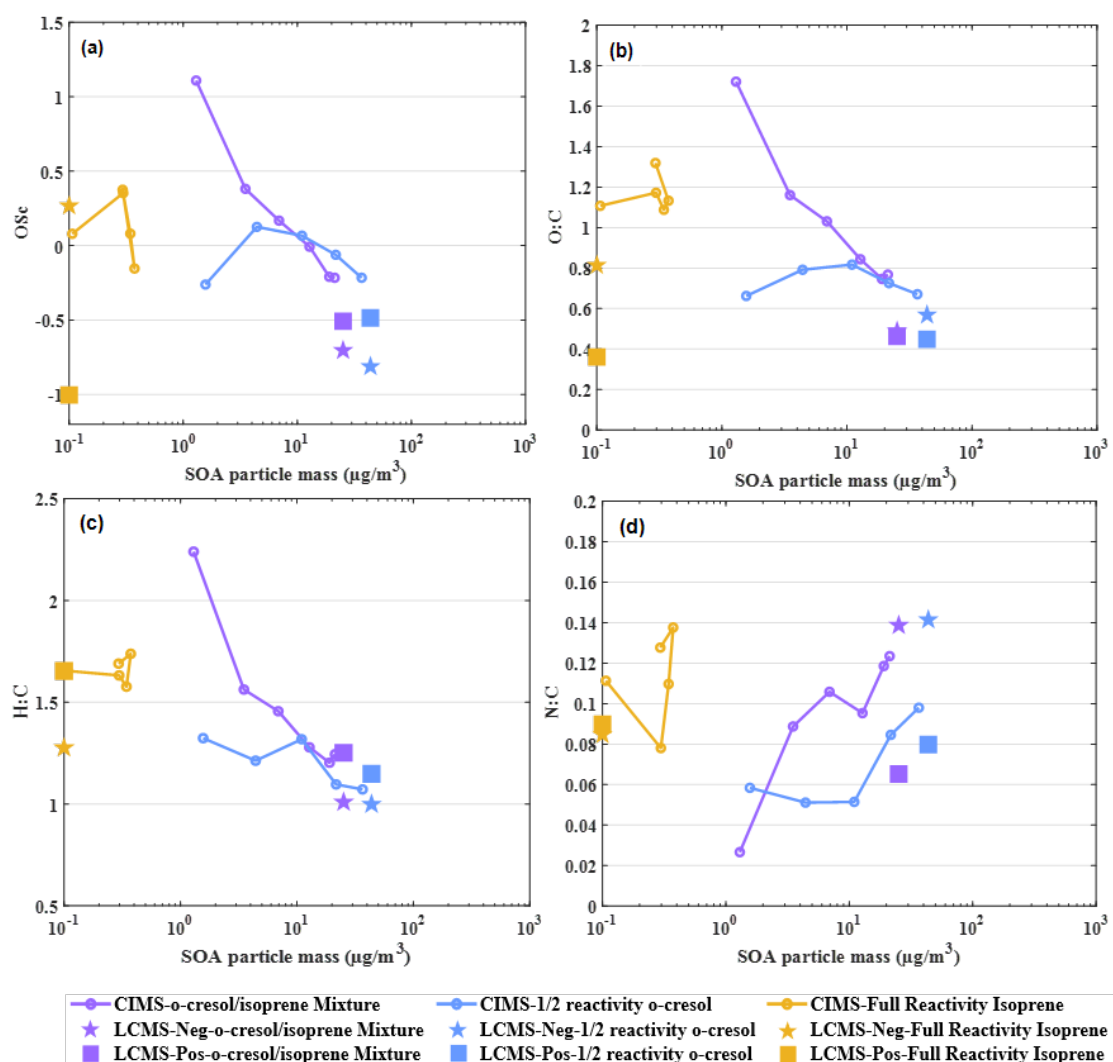


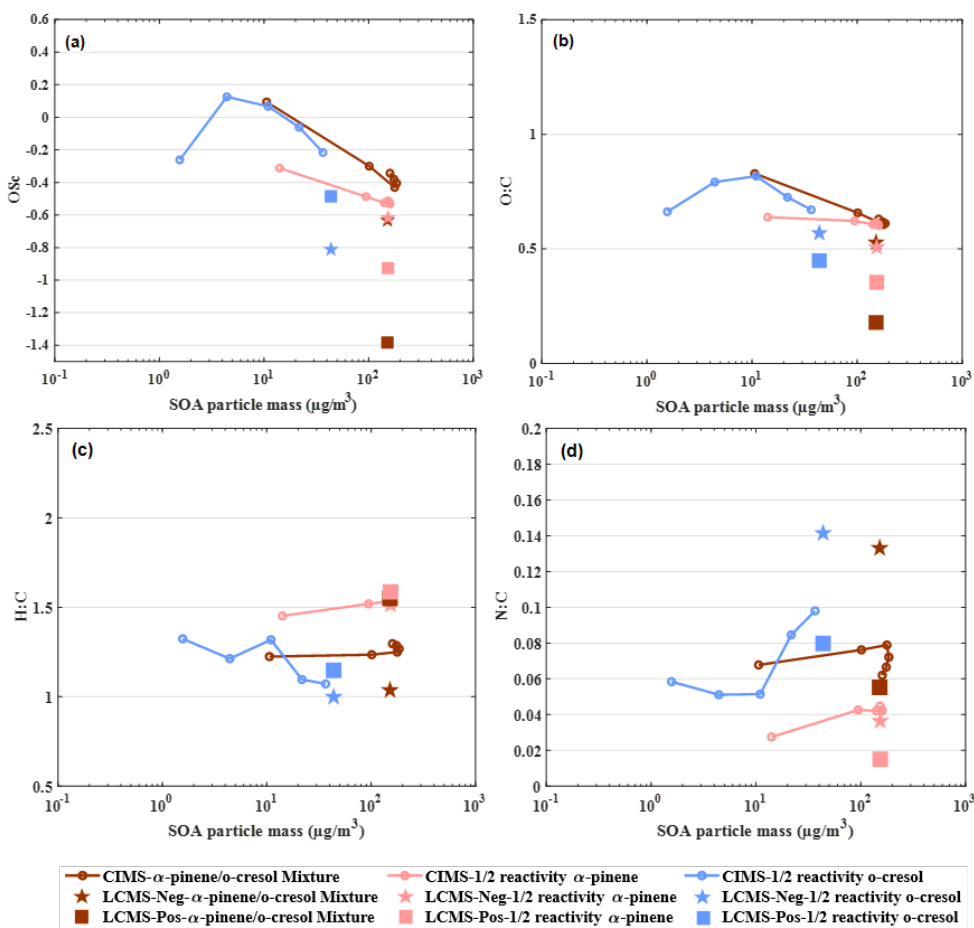


Figure 3: Evolution of SOA particle composition in terms of a) average carbon oxidation state (\overline{OSc}), b) O/C, c) H/C and d) N/C atomic ratios as function of SOA mass concentration from FIGAERO-CIMS and UHPLC-HRMS measurements (-ve Ionization Mode (Neg) and +ve ionization mode (Pos)) in binary *o*-cresol /isoprene mixture, ½ reactivity individual *o*-cresol and full reactivity individual isoprene experiments.

525 (c) *α -pinene & *o*-cresol Binary System*

Figure 4 shows the changes in \overline{OSc} , and atomic ratios (O/C, H/C and N/C) of SOA particles derived from FIGAERO-CIMS and UHPLC-HRMS in the binary α -pinene / *o*-cresol mixture and the individual ½ reactivity precursor experiments. Panel a) shows that FIGAERO-CIMS average \overline{OSc} decreases with SOA mass concentration above 3 $\mu\text{g}/\text{m}^3$ mass concentration in all experiments, though the \overline{OSc} is initially lower in the *o*-cresol experiment, driven by the low O/C. \overline{OSc} in the mixture system drop from 0.09 to -0.34 with increasing mass; a greater decrease than in the individual *o*-cresol ($\overline{OSc} = 0.12$ to -0.26) and α -pinene ($\overline{OSc} = -0.31$ to -0.51) experiments. Overall, the gradient in the mixture experiment is similar to the α -pinene experiment, but with an increase in the average degree of oxidation, though somewhat raised towards the *o*-cresol average \overline{OSc} by an increase in O/C. The O/C, H/C and N/C in the mixture system exhibit similar trends to the α -pinene experiment (Fig.4b,4c and 4d) with absolute values in the mixture midway between the α -pinene and *o*-cresol experiments (O/C falling from 0.82 to 0.63, N/C rising from 0.02 to 0.12, H/C modestly from 1.22 to 1.29).

540 The UHPLC-HRMS negative ionisation average \overline{OSc} and O/C ratio for the mixture were -0.63 and 0.52 respectively, comparable to those in the α -pinene experiment. Positive ionisation mixture \overline{OSc} and O/C ratio values were both lower than the two single precursor values (Fig.4a and 4b). H/C and N/C ratios of the mixture in positive ionisation mode were similar to the *o*-cresol experiment (H/C=1.55, and N/C = 0.55),



545

Figure 4: Evolution of SOA particle composition in terms of a) average carbon oxidation state \overline{OSc} , b) O/C, c) H/C and d) N/C atomic ratios as function of SOA mass concentration from FIGAERO-CIMS and UHPLC-HRMS measurements (-ve Ionization Mode (Neg) and +ve ionization mode (Pos)) in binary α -pinene / *o*-cresol mixture, $\frac{1}{2}$ reactivity individual α -pinene and $\frac{1}{2}$ reactivity individual *o*-cresol experiments.

550

(d) the ternary system

555

Figure 5 shows the change in average atomic ratios (O/C, H/C and N/C) and \overline{OSc} during SOA evolution in the ternary mixture system, along with $\frac{1}{3}$ reactivity α -pinene, $\frac{1}{3}$ reactivity isoprene and $\frac{1}{2}$ reactivity *o*-cresol experiments from FIGAERO-CIMS and UHPLC-HRMS measurements. The $\frac{1}{3}$ reactivity *o*-cresol data were not available owing to instrumental failure. Fig. 1c shows that the \overline{OSc} and atomic ratios are comparable between full reactivity and $\frac{1}{2}$ reactivity *o*-cresol



experiments and it is plausible to expect similar molecular concentrations and hence aggregate properties in particles formed in the $\frac{1}{2}$ and $\frac{1}{3}$ reactivity individual *o*-cresol experiments.

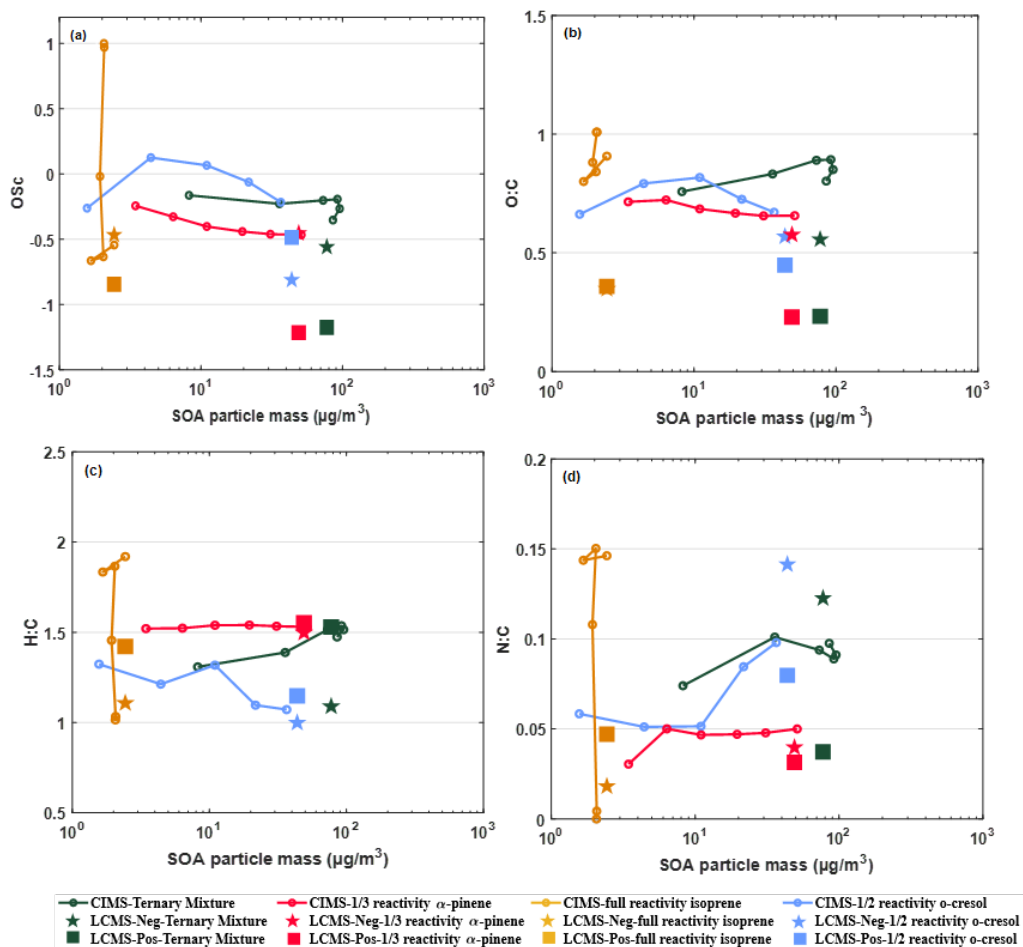
560 Panel a) shows FIGAREO-CIMS average \overline{OSc} in the ternary mixture (decreasing in degree of oxidation from -0.16 to -0.35) is between that in the α -pinene and *o*-cresol experiments, suggesting an influence from both precursors. Similarly, the mixture exhibits an average H/C ratio between the sole α -pinene and *o*-cresol experiment, increasing from 1.30 to 1.47 (Fig.5c). The O/C and N/C ratios in the ternary mixture system increased with mass (O/C: 0.75 to 0.80, N/C: 0.07 to 0.09) and

565 were higher than those in the α -pinene and *o*-cresol experiments (Fig.5b and 5d). Approximately $2\mu\text{g}/\text{m}^3$ of measurable products were generated in the $\frac{1}{3}$ reactivity single isoprene experiment. The average \overline{OSc} decreased from 1 to -0.54, possibly owing to the significant increase in the H/C and N/C ratios (H/C: 1 to 1.9, N/C: 0.004 to 0.14) while the O/C ratios were comparable (O/C: \sim 0.9) for the 6 hours experiments in $\frac{1}{3}$ reactivity single isoprene experiment.

570 The average \overline{OSc} in the α -pinene/ *o*-cresol binary mixture system (Brown line in Fig. 4a, $\overline{OSc} \cong 0.09$) are higher than the ternary mixture system in the early stage of experiment (Green line in Fig 5a, $\overline{OSc} \cong -0.16$), as obtained from the FIGAERO-CIMS though they have similar mass concentration ($\sim 10\mu\text{g}/\text{m}^3$).

UHPLC-HRMS average \overline{OSc} and O/C ratios were similar to those in the sole α -pinene

575 experiments in both ionisation modes. However, the H/C and N/C ratio in the ternary mixture (H/C=1.52, N/C=0.03) was comparable to the α -pinene experiment in positive ionisation modes. (Fig.5c and 5d), but closer to the *o*-cresol in negative. Also, the average \overline{OSc} and H/C ratios of ternary system were similar to those in the isoprene experiment in negative ionisation mode.



580

Figure 5: Evolution of SOA particle composition in terms of a) average carbon oxidation state \overline{OSc} , b) O/C, c) H/C and d) N/C atomic ratios as function of SOA mass concentration from FIGAERO-CIMS and UHPLC-HRMS measurements (-ve Ionization Mode (Neg) and +ve ionization mode (Pos)) in ternary α -pinene / *o*-cresol / isoprene mixture, $\frac{1}{3}$ reactivity individual α -pinene and $\frac{1}{2}$ reactivity individual *o*-cresol experiments.

585

3.3. Additional insight into \overline{OSc} through inclusion of HR-ToF-AMS data

590

This section presents a comparison of the average carbon oxidation state of SOA particles detected by HR-ToF-AMS, FIGAERO-CIMS and UHPLC-HRMS techniques from mixed precursors



systems and their corresponding single precursors experiments. Owing to the inability to reliably discern the N/C using the HR-ToF-AMS, the average carbon oxidation state presented in this section does not account for \overline{OS}_N calculated from all measurements. This allows for a comparison
595 of the compositional properties as measured by the three instruments, although these measurements are not directly comparable to those in section 3.2 that always has higher average \overline{OS}_c .

Fig.6a suggests that the average \overline{OS}_c of isoprene-derived compounds has only a modest influence on the carbon oxidation state in the binary α -pinene/isoprene system when calculated from all MS
600 measurements. HR-ToF-AMS derived \overline{OS}_c in the mixture is comparable to the individual α -pinene experiment at all particle mass concentrations and lower than the isoprene experiment (when only low particle mass was formed). Both systems exhibit an increase with SOA particle mass concentration up to $\sim 10 \mu\text{g m}^{-3}$, followed by reduction in the degree of oxidation as more mass was formed. The absolute values in the mixture (-0.33 to -1.15) were slightly lower than the
605 individual α -pinene values (-0.31 to -0.99). The FIGAERO-CIMS \overline{OS}_c in the mixture were also close to the α -pinene in trend and absolute values (-0.26 to -0.27) as were the UHPLC-HRMS average \overline{OS}_c in both ionisation modes with the negative ionisation value close to those from the final HR-ToF-AMS measurement and slightly lower than from the FIGAERO-CIMS.

HR-ToF-AMS measurements in Fig.6b show \overline{OS}_c of SOA formed in the *o*-cresol / α -pinene
610 binary mixture system falls between that of the SOA in the individual VOC experiments, indicating influence of oxidation products from both precursors. \overline{OS}_c in the mixture initially increases (from -1.13 to -0.30) before falling to -0.5 once the mass concentration had reached $10.8 \mu\text{g m}^{-3}$. A similar trend was seen in the $\frac{1}{2}$ reactivity α -pinene experiment at a lower \overline{OS}_c value. The FIGAERO-CIMS \overline{OS}_c in all systems was higher than the HR-ToF-AMS \overline{OS}_c , in the mixture ($\overline{OS}_c = 0.43$
615 to -0.03) and α -pinene experiments ($\overline{OS}_c = -0.17$ to -0.29) following the same reducing trend, whilst the *o*-cresol \overline{OS}_c increased to a plateau in both HR-ToF-AMS and FIGAERO-CIMS analyses. The UHPLC-HRMS \overline{OS}_c of SOA in the mixture was -1.19 in positive ionisation mode, lower than both the α -pinene ($\overline{OS}_c = -0.87$), and *o*-cresol ($\overline{OS}_c = -0.25$) experiments. Negative mode \overline{OS}_c in the mixture was 0.02, which is 0.11 lower than for *o*-cresol and 0.52 higher than
620 for α -pinene (Fig.6b).



Fig.6c shows that the average \overline{OSc} of isoprene-derived compounds also only exert a modest influence on that of the binary *o*-cresol/isoprene binary mixture in measurements from all MS techniques. The HR-ToF-AMS measured \overline{OSc} in the mixture is comparable to that in the $\frac{1}{2}$ reactivity *o*-cresol experiment, both increasing from -1.2 to 0.3 at $\sim 15 \mu\text{g m}^{-3}$ thereafter slightly increasing in the mixture system (Fig.6c). The FIGAERO-CIMS \overline{OSc} in the mixture decreased from 1.2 to 0.2 with mass concentration increasing from $1.3 \mu\text{g m}^{-3}$ to $21.2 \mu\text{g m}^{-3}$, whilst the single *o*-cresol \overline{OSc} increased from 0 to 0.27 across the same range of mass concentration, all values being higher than the HR-ToF-AMS \overline{OSc} until the highest mass concentrations. The \overline{OSc} in the mixture is comparable though slightly lower than that in the single *o*-cresol experiment after 6- hours in both ionisation mode of UHPLC-HRMS measurements.

Fig.6d shows that the average \overline{OSc} in the ternary mixture from HR-ToF-AMS increased marginally from -0.44 to a maximum of -0.22 with a mass concentration of $11.84 \mu\text{g m}^{-3}$, followed by a gradual decrease to -0.52. The single VOC $\frac{1}{3}$ reactivity α -pinene experiment showed a strong increase in \overline{OSc} from -2.51 to -0.66 and the $\frac{1}{2}$ reactivity *o*-cresol experiment more gradually increasing from -1.2 to a plateau of 0.3 at $\sim 15 \mu\text{g m}^{-3}$. The average \overline{OSc} is around -1.7 in the $\frac{1}{3}$ reactivity isoprene experiment with stable mass concentration of approximately $1 \mu\text{g m}^{-3}$ for 6 hours experiment. The FIGAERO-CIMS average \overline{OSc} in for all experiments was consistently higher than the HR-ToF-AMS measurements as a function of SOA particle mass concentration. Moreover, the oxidation state in the ternary mixture experiment (0.13 to 0.2) was higher than that of the α -pinene experiment but slightly lower than or comparable to the *o*-cresol experiment (0 to 0.2). Negative ionisation mode UHPLC-HRMS measurements showed the average ternary system \overline{OSc} to be similar to that in the *o*-cresol experiment, but positive mode was more comparable to that in the α -pinene experiment. The average \overline{OSc} in the ternary mixture system as obtained from all instruments was dissimilar to that in the $\frac{1}{3}$ reactivity isoprene experiment. Additionally, it is noteworthy that Fig.6 demonstrates good agreement between the negative ionisation mode results and the FIGAERO-CIMS measurements across all experiments.

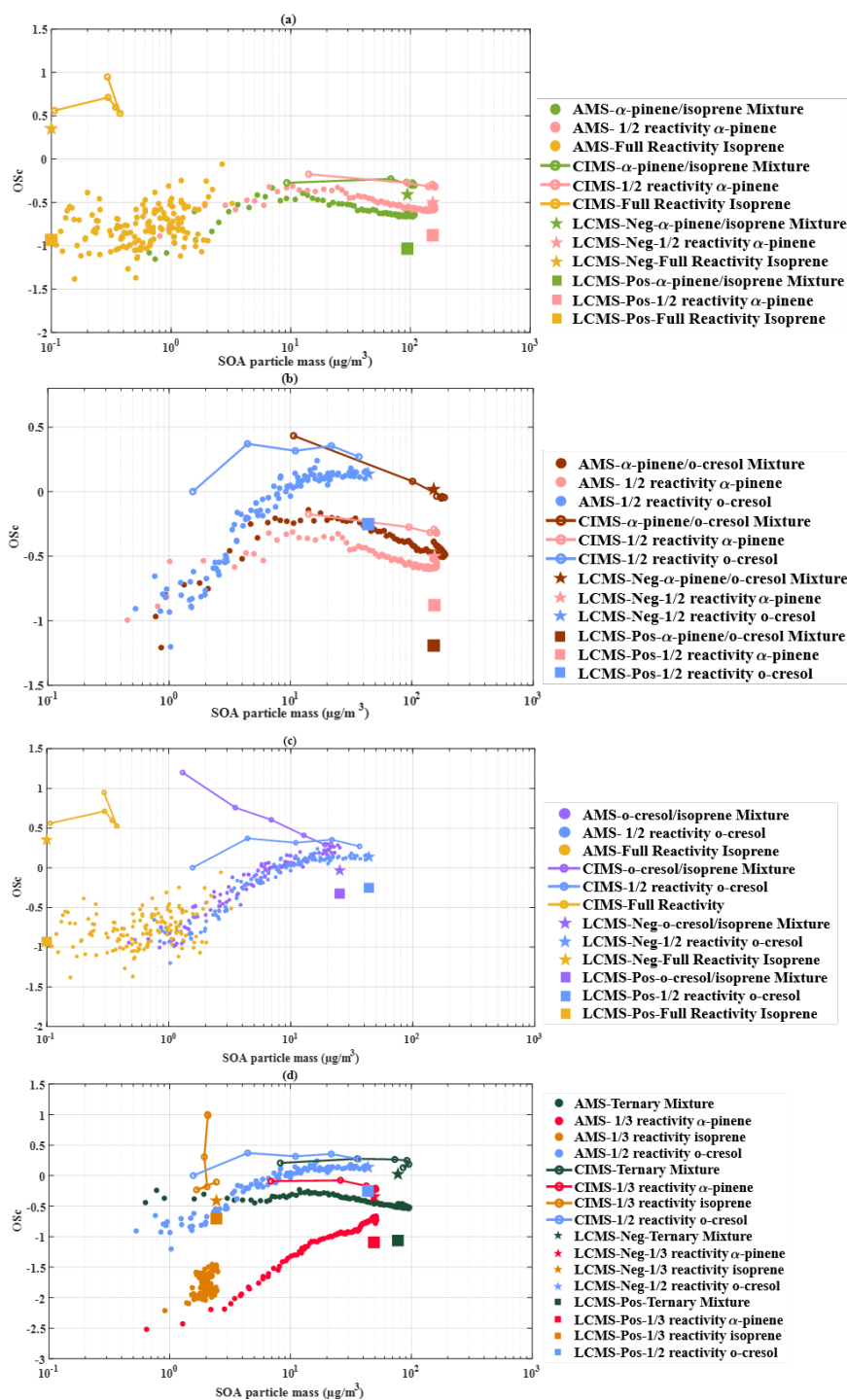




Figure 6: \overline{OSc} plotted as a function of SOA particle mass concentration in mixed precursor systems, a) binary α -pinene /isoprene system; b) binary α -pinene / *o*-cresol system; c) isoprene/*o*-cresol system, d) Ternary mixture precursor system from HR-ToF-AMS, FIGAERO-CIMS and UHPLC-HRMS measurements (Negative Ionization Mode (Neg) and Positive ionization mode (Pos)).

4. Discussion

4.1. The application of multiple mass spectrometric techniques to the average oxidation state of carbon in SOA particles

In this study, the average carbon oxidation state of SOA from different precursor systems was estimated from three mass spectrometry techniques measurements. The combination of online and offline mass spectrometric techniques to estimate the average \overline{OSc} of complex organic mixtures has not been widely adopted, particularly in the context of SOA components from the oxidation of mixed precursors in atmospheric simulation chamber studies. Each technique has its own strengths and limitations. The electrospray ionisation method used in the UHPLC-HRMS extraction can provide exact elemental ratios of individual compounds within organic mixtures using small sample volume. The FIGAERO-CIMS can provide molecular information for hundreds of particulate compounds in hourly timescale throughout a chamber experiment, with the low instrument backgrounds enabling detection limits in the picogram m^{-3} range for particle phase organic species (Lopez-Hilfiker et al., 2014) The average \overline{OSc} from FIGAERO-CIMS was determined using 6 measurements from the six thermal desorption cycles throughout each experiment, whilst the UHPLC-HRMS values were derived from analyses of filters collected at the end of each experiment. Both the UHPLC-HRMS and FIGAREO-CIMS techniques are selective ionisation technique, with different response factor toward widely various components that may bias the average \overline{OSc} estimation. For instance, the negative ionisation mode in UHPLC-HRMS technique exhibits high sensitivity towards nitro-aromatic compounds (Shao et al., 2022a). Low-volatility molecules may experience thermal decomposition in the FIGAREO-CIMS leading to fragmentation, influencing the average \overline{OSc} estimation (Du et al., 2021). The HR-ToF-AMS allows entire ensemble of SOA particles to be detected, fully fragmenting the flash vapourised particles by electron impact ionisation and measuring the elemental ratios in real time. This is the



possible reason that we observed values of the FIGAERO-CIMS average \overline{OSc} were higher than the HR-ToF-AMS values and UHPLC-HRMS value in both single precursors' experiment (Fig.1b
685 and 1d). The negative mode UHPLC-HRMS value in these two single precursors system is more comparable to HR-ToF-AMS value, but the positive mode UHPLC-HRMS values were lower. However, the accuracy of the retrieved elemental ratios is affected by uncertain empirical corrections in the analysis. Probably more importantly the average \overline{OSc} estimation obtained from our HR-ToF-AMS measurement cannot account for $\overline{OS_N}$ given the limited resolution of the
690 instrument calibrations. Farmer et al. (2010) reported the potential for overestimation of N and underestimation of O in ambient measurements by HR-ToF-AMS, highlighting the need for high-quality m/z calibrations and peak width/shape parameters when attempting to quantify nitrogen-containing compounds in HR-ToF-AMS spectra.

695 There are significant differences between carbon oxidation state (not accounting for $\overline{OS_N}$) derived from the FIGAERO-CIMS measurements and those from HR-ToF-AMS under the same SOA mass concentration in all single experiments (Figs.1b and 1d) and mixed precursor systems (Fig.6 and Fig.1). The carbon oxidation state in FIGAERO-CIMS estimation is substantially higher than that in the HR-ToF-AMS measurement. The FIGAERO-CIMS used iodine as reagent ion, with an
700 inherently higher sensitivity toward to the oxygenated organic compounds, biasing the measurements towards oxidized organic species (Lee et al., 2014). There is an additional possibility that thermal decomposition fragments may form from the larger organic molecules during the filter thermal desorption in the FIGAERO-CIMS that may potentially result in higher \overline{OSc} than their parent molecules. The average carbon oxidation state from FIGAERO-CIMS will
705 depend on a subset of compounds biased towards higher oxidation state and consequently will be higher than that derived from HR-ToF-AMS and UHPLC-HRMS measurements. On the other hand, the average \overline{OSc} in the binary *o*-cresol/isoprene precursor system was high at the early stage of experiment (Fig.6c), possibly indicating that the presence of isoprene influenced the early stages of the chemistry, though this requires further investigation. There is a substantial difference of
710 average carbon oxidation state in the single VOC isoprene experiments (Fig.6a and 6c), likely resulting from potential artefacts in the instruments and filter background since there was an insufficient amount of SOA particle mass produced in these experiments and the collected filter mass loading was low.



715 As stated, the average \overline{OSc} comparisons with the HR-ToF-AMS discussed above do not account
for the oxidation state of nitrogen ($\overline{OS_N}$) and sulfur ($\overline{OS_S}$) in their calculation. However,
Organosulfate (CHONS and CHOS) and organonitrate (CHON and CHONS) have been reported
in chamber experiments with NO_x and ammonium sulphate (Surratt et al., 2007; Surratt et al., 2008;
Bruns et al., 2010; Fry et al., 2009). The heteroatom-containing groups will clearly impact on the
720 derived \overline{OSc} which should therefore be determined from 2O/C-H/C-xN/C-yS/C, where x and y
refer to the oxidation states of nitrogen ($\overline{OS_N}$) and sulphur ($\overline{OS_S}$) (Kroll et al., 2011). The
uncertainty in HR-ToF-AMS \overline{OSc} determination associated with S-containing groups is likely to
be minimal since the S atom in weakly-bound species, such as organosulphates, tend not to be
measured under thermal methods. This is not the case with nitrogen-containing compounds which
725 may affect \overline{OSc} determination, but unambiguous attribution of N is challenging at the limited
resolution of the technique. Additionally, neutral losses can occur in the HR-ToF-AMS during
thermal desorption, as some thermally labile or highly volatile compounds can desorb as neutral
fragments (e.g., CO₂ or H₂O). This can lead to an underestimation of certain oxygenated or
heteroatom-containing species, biasing the measured elemental ratios (e.g., O:C and N:C) and
730 adding uncertainty to the calculated average \overline{OSc} .

The $\overline{OS_N}$ of CHON compounds in FIGAERO-CIMS measurements clearly influenced the signal-
weighted average \overline{OSc} , consequently reducing the average \overline{OSc} . The UHPLC-HRMS derived
 \overline{OSc} is similarly influenced, particularly in *o*-cresol containing systems in negative ionisation
735 mode (owing to an enhanced sensitivity to specific CHON species likely formed through NO₂+OH
radical reactions, dominated by nitro-aromatics as reported in Shao et al., 2022a) and the average
 \overline{OSc} is significantly lower when accounting for $\overline{OS_N}$.

740 **4.2. Comparison of SOA average Carbon Oxidation State at various precursor VOC concentration**

The calculated carbon oxidation state of particles in the single precursor systems that generated
significant mass (α -pinene and *o*-cresol) with their initial concentration were compared. The initial
745 “full” iso-reactive (accounting for their reactivity towards OH) concentration of the α -pinene and



o-cresol were 309 and 400 ppb. Experiments with half- and third- of these initial concentrations were also conducted to enable total initial iso-reactivity in the binary and ternary mixtures system. Further details can be found in Voliotis et al. (2022b).

FIGAERO-CIMS average \overline{OSc} from the α -pinene experiments accounting and not accounting for $\overline{OS_N}$ is shown in Fig.1a and 1b, showing comparable values at all mass concentrations. In the HR-ToF-AMS initial $\frac{1}{2}$ reactivity α -pinene experiment showed a higher average \overline{OSc} than full initial reactivity α -pinene experiment, which was in turn higher than that from the $\frac{1}{3}$ reactivity experiment (Fig.1b). It should be noted that the NO_x concentration was reduced along with reduction of VOC initial concentration in half-reactivity experiment in order to maintain a comparable VOC/ NO_x ratio across the system. This will influence the oxidant conditions, though it is unclear precisely why the oxidation state is so divergent at the lower particle mass concentrations within initial VOC concentration.

Unlike the α -pinene precursor, the average \overline{OSc} in the single precursor *o*-cresol experiment seems independent of initial precursors concentration in both HR-ToF-AMS and FIGAERO-CIMS measurement, whether or not $\overline{OS_N}$ is considered (Fig.1b and 1d). The degrees of oxidation of organic species appear comparable irrespective of initial *o*-cresol and NO_x concentration. This might be due to the negligible reactivity of *o*-cresol towards O_3 (Atkinson, 2004). It should be noted that there is difficulty in reporting the O_3 direct measurement by UV absorption in the single precursor *o*-cresol experiment in this study owing to the UV absorption by *o*-cresol and its oxidation products. More details about the O_3 measurement by UV absorption was influenced by UV absorption by *o*-cresol was mentioned in the Voliotis et al. (2022b). However, this independence is less clear in the UHPLC-HRMS data, where a noticeably larger drop in average \overline{OSc} was observed in the $\frac{1}{2}$ reactivity experiment when the $\overline{OS_N}$ was included. This implies that CHON species, particularly highly oxidized, which may contribute more significantly to the overall composition under lower SOA mass loading.

Additionally, when the $\overline{OS_N}$ is accounted for, the \overline{OSc} drop in the UHPLC-HRMS negative ionisation mode is larger than in FIGAERO-CIMS, especially in the $\frac{1}{2}$ reactivity experiment ($\delta \overline{OSc} = 0.95$ vs 0.48, respectively). This suggests that UHPLC-HRMS negative mode is more sensitive to CHON species that might highly be oxidized in low-mass systems. In contrast, the full reactivity experiment shows a greater drop in FIGAERO-CIMS ($\delta \overline{OSc} = 0.58$) than in UHPLC-



HRMS ($\delta \overline{OSc} = 0.70$), possibly reflecting greater sensitivity of FIGAERO-CIMS to semi-volatile nitrogen-containing species at higher SOA mass.

780 **4.3. Comparison of SOA average Carbon Oxidation State accounting for $\overline{OS_N}$ in mixtures**

The average \overline{OSc} taking into account the $\overline{OS_N}$, H/C, O/C and N/C ratios in the mixtures (three binary and the ternary precursor system) and the corresponding single precursor systems were
785 compared using the FIGAERO-CIMS and UHPLC-HRMS data.

(a) α -pinene /isoprene binary mixture system

The $\frac{1}{2}$ reactivity single precursor α -pinene experiment was used as reference experiment for binary
790 mixtures containing α -pinene, since it made a half contribution to the VOC reactivity. The trend of average \overline{OSc} in the α -pinene /isoprene mixture system was comparable to that in the $\frac{1}{2}$ reactivity α -pinene experiments, suggesting that the dominant control by α -pinene oxidation products (Fig.2a). This is unsurprising given the high established α -pinene particle mass yield from OH oxidation in the presence of seed particles (Ahlberg et al., 2017; Eddingsaas et al., 2012; Henry et al., 2012). However, the magnitude of average \overline{OSc} in mixture system is slightly lower
795 than in the single α -pinene experiment, the influence of isoprene oxidation products on the average carbon oxidation state of total SOA. Isoprene is known to form C₄ and C₅ compounds with high volatility (e.g. methacrolein (C₄) and C₅-hydroxycarbonyls) on OH oxidation, with potential to suppress the particulate mass form from α -pinene oxidation in the mixed system (Wennberg et al.,
800 2018; Stroud et al., 2001; Carlton et al., 2009) (more information in section 4.5). Another possible interpretation is that the isoprene driven products (semi-volatile) partitioning in the mixture system due to high amount of adsorptive mass generated from the precursor α -pinene, leading to lower the average \overline{OSc} in the binary α -pinene/isoprene system compared to single $\frac{1}{2}$ reactivity α -pinene experiment. According to Voliotis et al. (2022a), the products resulting from isoprene contribute
805 approximately 3% of the total signal observed in the measurement conducted with the FIGAERO-CIMS instrument in the binary α -pinene/isoprene system. The difference in N/C ratios between $\frac{1}{2}$ reactivity α -pinene experiment and the binary mixture contributed to the difference in average \overline{OSc} and the H/C and O/C ratios were similar (Fig.2b and 2c), with N/C increasing with SOA



particle mass in both systems. This suggests an increasing contribution of CHON compounds in
810 both systems, with an increased contribution in the presence of isoprene.

(b) *o*-cresol/Isoprene binary mixture system

The FIGAERO-CIMS \overline{OSc} in the binary *o*-cresol/isoprene mixtures shared a broadly similar trend
815 with the $\frac{1}{2}$ reactivity single precursor *o*-cresol experiment. In addition, the binary mixture system
has generally higher magnitude than the $\frac{1}{2}$ reactivity single precursor *o*-cresol experiment apart
from the measurement in the first half-hour of the experiment. However, \overline{OSc} in the binary *o*-
cresol/isoprene mixtures showed little similarity to the isoprene experiment \overline{OSc} (Fig.3a),
suggesting a strong dependence on the *o*-cresol oxidation products. On the other hand, in the
820 early stage of experiment (relatively low SOA mass), there is a high average \overline{OSc} in the binary
system driven by the high O/C and low N/C compared to the $\frac{1}{2}$ reactivity *o*-cresol experiment.
This indicates an influence of isoprene at the early stages of the oxidation that could be a subject
of further investigation. Whilst details of the mechanistic origins of this influence are unclear, Shao
et al (2022a) report compounds uniquely found in this mixed system, but not in the oxidation of
825 the individual precursors. Additionally, a clear divergence is observed between the N:C results in
positive and negative ionisation modes obtained from UHPLC-HRMS (Fig.3d). This is likely due
to the contribution of nitro-aromatic compounds generated from *o*-cresol oxidation, which are
sensitively detected in negative ionisation mode.

830 (c) α -pinene /*o*-cresol binary mixture system

The average FIGAERO-CIMS \overline{OSc} in the binary α -pinene / *o*-cresol system exhibited a similar
trend to that in the $\frac{1}{2}$ reactivity α -pinene experiment at a higher magnitude, more comparable to
that of the $\frac{1}{2}$ reactivity *o*-cresol experiment (Fig.4a). This indicates that both α -pinene and *o*-cresol
835 contribute non-negligibly to the average \overline{OSc} in the mixture. According to the findings of Voliotis
et al. (2021), the FIGAERO-CIMS demonstrated high sensitivity towards CHON products
resulting from the oxidation of *o*-cresol. This high sensitivity might explain why the binary
 α -pinene/ *o*-cresol system shows a comparable magnitude of \overline{OSc} with the single $\frac{1}{2}$ reactivity *o*-
cresol system, despite α -pinene being recognized as a precursor with higher SOA yield.



840 The O/C ratio contributed to the difference in \overline{OSc} (Brown line in Fig.4b,4c and 4d) more
significantly than the H/C and N/C ratios. The O/C reduced with SOA particle mass, whilst H/C
and N/C ratios remained constant, implying oxygen atoms loss (e.g. $RO_2+R'O_2$ termination
reactions) during the SOA production. Furthermore, the difference in \overline{OSc} could be influenced
845 making a significant contribution. Voliotis et al. (2021) reported FIGAERO-CIMS measurement
of products uniquely found in this α -pinene/*o*-cresol experiment, with the majority of these unique-
to-mixture compounds having $nC=5-10$ and $nC>10$. UHPLC-HRMS measurements reported in
Shao et al., (2022a) also showed that high carbon number compounds contribute significantly in
positive ionisation mode, likely cross-products from α -pinene and *o*-cresol oxidation in either gas
850 or particle-phase.

(d) The ternary mixture

855 The FIGAERO-CIMS average \overline{OSc} in the ternary mixture does not follow a similar trend to any
single VOC experiment (Fig.5a). The \overline{OSc} in this mixture was higher than in the α -pinene, but
lower than *o*-cresol experiment, and the average \overline{OSc} is likely not controlled by any single
precursor. The trends in average atomic ratios (O/C, H/C and N/C) also have little similarity to
those in the individual experiment (Fig.5b,5c and 5d), implying contributions from each of them.
860 In the first half-hour of the experiment, the average \overline{OSc} obtain from FIGAERO-CIMS in the
ternary mixture was lower than in the α -pinene/*o*-cresol binary mixture though both systems
generated similar SOA particle mass concentration (Fig.5a). This may result from the early
involvement of isoprene as an OH scavenger in the early stage of the experiment, leading to
suppression of the low volatility and highly oxygenated products formed from α -pinene and *o*-
865 cresol oxidation. Oxidation in the ternary mixture may involve complex reactions that include
interaction between radicals from the three individual precursors and alterations in the oxidation
pathways of the individual precursors. The UHPLC-HRMS measurements in both ionisation
modes further support the contention that each VOC contributes to the chemical composition in
the ternary mixture, influencing the average carbon oxidation state, in addition to products
870 uniquely found in the mixture (Fig.S1).



4.4. Comparison of average Carbon Oxidation State ignoring $\overline{OS_N}$ in the mixtures

This section assesses the influence of individual precursors on $\overline{OS_C}$ in mixtures without accounting for $\overline{OS_N}$ using HR-ToF-AMS, FIGAERO-CIMS and UHPLC-HRMS measurements.

875 In binary isoprene-containing mixtures, the $\overline{OS_C}$ from all three instruments showed no clear similarity to the full reactivity isoprene experiment (Fig.6a and 6c), in agreement with the values accounting for $\overline{OS_N}$ (Fig .2a and 3a). α -pinene and *o*-cresol products controlled $\overline{OS_C}$ in their respective mixtures with isoprene. The ternary mixture again displayed a non-additive behaviour, with average $\overline{OS_C}$ values falling between those of α -pinene and *o*-cresol, similar to the α -pinene /
880 *o*-cresol binary mixture (Fig.6d). The trend in HR-ToF-AMS $\overline{OS_C}$ in the α -pinene / *o*-cresol binary mixture most closely followed that of the α -pinene experiment but increased slightly towards that of *o*-cresol (Fig.6b). Both *o*-cresol and α -pinene products likely contributed to the average $\overline{OS_C}$ in their binary mixture, but possibly more from α -pinene. The FIGAERO-CIMS $\overline{OS_C}$ presents a contrary picture, with the trend following that of α -pinene, but absolute value closer to that of *o*-
885 cresol.

4.5. Drivers for carbon oxidation state behaviour

Knowing the oxidation pathway of precursors provides a description of the chemical behaviour of the mixed systems controlling average carbon oxidation state during SOA formation and evolution. The oxidant regime (OH and O₃) during the experiments can differ between the mixture and
890 individual precursor experiments despite our best attempts to maintain similar conditions through initial “iso-reactivity” as explained in Voliotis et al. (2022b). The ozone production and hence OH profile may not be the same in the mixture as in the individual precursor experiments and the reactivity towards the available oxidants will not remain equal. This, in turn, will lead to changes in the timescale of product formation from each of the reactants. Both α -pinene and isoprene are
895 readily oxidized by both OH and O₃, while the *o*-cresol is unreactive towards O₃ owing to its stable aromatic ring and lack of double bond. This section discusses the drivers causing different carbon oxidation state between single and mixture precursors system with reference to the various classes of potential reactions (e.g. functionalization oligomerization, and fragmentation).



The FIGAREO-CIMS results suggest that the carbon oxidation state profile accounting for \overline{OSN} is higher in single α -pinene experiment compared to its mixture with isoprene (Fig.2a), but carbon oxidation state profile is similar if \overline{OSN} is not considered (Fig.6a). Fig. 6a also shows that the HR-ToF-AMS average \overline{OSc} in the mixture is lower than in the individual α -pinene experiment. Voliotis et al. (2022a) reported that the binary α -pinene/isoprene system exhibits a lower SOA mass yield compared to the sole α -pinene experiment. While this may initially suggest a suppression in the formation of low-volatility α -pinene oxidation products due to competition for oxidants, Voliotis et al. (2022a) showed that the volatility distribution of the SOA from the α -pinene/isoprene mixture was comparable to that from the α -pinene-only experiment. This might be attributed to the formation of new products in the mixture, which had similar volatility characteristics to those from the α -pinene SOA. However, the chemical composition was distinctly altered, with some α -pinene products being suppressed and unique compounds forming in the presence of isoprene. These changes in chemical composition, rather than volatility, may help explain the observed decrease in average carbon oxidation state and SOA mass in the mixed system.

In the isoprene / *o*-cresol system, the average \overline{OSc} derived from both online and offline mass spectrometry were comparable to that obtain in the individual *o*-cresol experiment, apart from the early state of FIGAERO-CIMS measurement, as discussed in section 4.3 (b) (Fig.3a and 6c). The wall-loss corrected particle mass in the mixture was lower than in the *o*-cresol experiment (as reported by Voliotis et al. (2022b)). This may be a result of the isoprene scavenging the available OH oxidants in the binary precursor system or reacting with O₃ which would otherwise have been available to form OH, both effects leading to reducing the SOA particle mass concentration from *o*-cresol oxidation (Voliotis et al., 2022b). A similar average \overline{OSc} was observed between the two systems, which is reasonable since the chemical composition of SOA formed from binary isoprene / *o*-cresol system show strong resemblance the single *o*-cresol experiment, with the dominance of CHON compounds with seven carbon atoms (C₇H₇NO₃, and C₇H₇NO₄ compounds) as identified by FIGAREO-CIMS and UHPLC-HRMS (Shao et al., 2022a; Voliotis et al., 2022a). Initially, it was hypothesized that isoprene might act as an OH scavenger, thereby limiting *o*-cresol oxidation, as seen in other systems such as α -pinene/isoprene mixtures. However, the similar average \overline{OSc} values between the single precursor *o*-cresol and binary *o*-cresol/isoprene systems suggest that this may not be play a dominant role in this case. A plausible explanation is the



presence of elevated ozone in the binary system, which will lead both to increased production of
930 OH via O_3 photolysis and to increased consumption of isoprene and possibly *o*-cresol oxidation
products (see Fig. S2 in [Voliotis et al., 2022b]). Additionally, unique-to-mixture products are
formed in the binary *o*-cresol/isoprene system, which may also contribute to the average \overline{OSc} in
the binary system (Voliotis et al., 2022a, Shao et al., 2022a). These explanations remain
speculative and highlight the need for mechanistic studies investigating the SOA formation in this
935 particular binary system.

In the binary α -pinene / *o*-cresol system, the FIGAERO-CIMS and HR-ToF-AMS carbon
oxidation states have a similar trend to the individual α -pinene experiment though the absolute
value in the mixture was between the *o*-cresol and α -pinene values whether accounting for \overline{OS}_N
or not in all instruments (Fig.4a and Fig.6b). Mixing *o*-cresol with α -pinene will increase the
940 degree of oxidation at any given mass loading and enhancing the average \overline{OSc} compared to single
 α -pinene experiment. These products may be partially attributed to formation of gaseous cross-
product formation from α -pinene and *o*-cresol followed by condensation in the mixed system.
More molecular information about the cross-products formation and potential mechanistic
differences between the mixtures and individual precursor experiment leading to compounds
945 uniquely found in the binary α -pinene/*o*-cresol mixture have been reported by Voliotis et al. (2021)
and (Shao et al., 2022a)

In the ternary mixture, the absolute magnitude of the average carbon oxidation state was between
the individual *o*-cresol and α -pinene experiments. The average \overline{OSc} of the ternary system is
similar to the binary *o*-cresol/ α -pinene system, but the trend with SOA particle mass concentration
950 was not the same as in any individual precursor experiment (Fig.5, and Fig.6d). This may be
attributed to the more complex chemistry in ternary system. Both *o*-cresol and α -pinene derived
products contributed to the chemical composition as Shao, et al, (2022a) reported, with negligible
contribution of isoprene driven products. This would lead to the average \overline{OSc} in ternary mixture
being higher than that in the individual α -pinene experiment with more oxygenated compounds
955 being *o*-cresol oxidation products. Meanwhile, the significant higher SOA particle mass in ternary
mixture compared to any single precursor experiment (single 1/3 reactivity α -pinene, single 1/2
reactivity *o*-cresol and 1/3 reactivity isoprene) might partially attributed to the formation of
gaseous cross-products that subsequently condense. This is consistent with both Voliotis et al.



(2021) and Shao et al. (2022a) who reported that compounds uniquely found in the mixture made
960 non-negligible contribution in ternary system. This cross-interaction between molecules might
include $\text{RO}_2 + \text{R}'\text{O}_2$ termination reactions (oxygen atoms loss process as we mentioned in 4.3)
leading to generate an increase in less oxygenated organic species, reducing average $\overline{\text{OSc}}$ during
particulate matter formation.

965 5. Summary

The average carbon oxidation state and atomic ratios (H/C, O/C and N/C) of SOA formed from
photooxidation of α -pinene, isoprene, *o*-cresol and their binary and ternary mixtures in the
presence of NO_x and ammonium sulphate seed particles was determined by HR-ToF-AMS,
970 FIGAERO-CIMS and UHPLC-HRMS. Factors affecting the average $\overline{\text{OSc}}$ during SOA evolution
in mixed precursor systems were interrogated by combining these online and offline mass
spectrometer measurements.

The average $\overline{\text{OSc}}$ obtained from FIGAERO-CIMS and UHPLC-HRMS were calculated both
975 accounting for, and not accounting for $\overline{\text{OS}_N}$. $\overline{\text{OS}_N}$ was inaccessible to the HR-ToF-AMS due to
its limited resolution and hence average $\overline{\text{OSc}}$ did not account for $\overline{\text{OS}_N}$. Average $\overline{\text{OSc}}$ not
considering $\overline{\text{OS}_N}$ showed substantial difference between the FIGAERO-CIMS, HR-ToF-AMS
and UHPLC-HRMS measurements, with the FIGAERO-CIMS and UHPLC-HRMS only
measuring a subset of compounds. The FIGAERO-CIMS has higher sensitivity toward more
980 oxygenate compounds, and UHPLC-HRMS has a particularly high sensitivity to aromatic nitro-
compounds in negative ionisation mode.

The average carbon oxidation obtained from FIGAERO-CIMS and UHPLC-HRMS appears
unaffected by the initial precursor concentration in the single precursor α -pinene experiments,
showing comparable magnitude in all three experiments (Full, $\frac{1}{2}$ and $\frac{1}{3}$ reactivity). By contrast,
985 the average $\overline{\text{OSc}}$ was influenced by the initial concentration of precursor in the single α -pinene
experiment obtained from the HR-ToF-AMS. The full reactivity of α -pinene has lower $\overline{\text{OSc}}$ (not
accounting for $\overline{\text{OS}_N}$) during SOA evolution than $\frac{1}{2}$ reactivity α -pinene, but higher than $\frac{1}{3}$



reactivity experiment. The underlying causes of these differences are not yet well understood and require further investigation.

990 The average \overline{OSc} (not accounting for $\overline{OS_N}$) in single precursor *o*-cresol experiment was not dependent on the initial concentration of precursor. CHON compounds have a significant influence on average \overline{OSc} of SOA in both the single VOC α -pinene and *o*-cresol experiments, since the average \overline{OSc} (accounting for $\overline{OS_N}$) has lower value than \overline{OSc} (not accounting for $\overline{OS_N}$).

The isoprene experiments generating insignificant SOA particle mass (with total concentration in
995 the full reactivity experiment never exceeding $1\mu\text{gm}^{-3}$) and so the trends in oxidation state were inaccessible. Isoprene only has a minor influence on the average carbon oxidation state of the SOA particles in the *o*-cresol/isoprene binary mixture, both trend and magnitude being almost identical to those in the single precursor *o*-cresol system. In contrast, the oxidation state decreased on
1000 addition of isoprene to α -pinene, with the average in the α -pinene/isoprene lower than the α -pinene value. This may result from isoprene scavenging OH leading to suppression of low volatility α -pinene driven oxygenated product formation. The degree of oxidation in the α -pinene / *o*-cresol system was complex since both precursors generated considerable SOA mass, and \overline{OSc} was affected by both precursors, with products from both α -pinene and *o*-cresol impacting on the oxidation state in the mixture. The \overline{OSc} shared similar trend with the sole α -pinene experiment,
1005 with an increase in absolute value towards that of *o*-cresol. Compounds uniquely found in the mixture contributed to this behaviour. In the ternary precursor system, no single precursor dominated the oxidation state, though the general pattern was similar to that in the α -pinene / *o*-cresol mixture. However, the addition of isoprene into ternary system leading to lower average carbon oxidation state compared to the α -pinene / *o*-cresol binary system in the early stage of
1010 experiment, which may result from isoprene acting as OH scavenger in the same way as the α -pinene/isoprene binary system.

This current study makes important first steps in the investigation of oxidation state in mixtures of SOA precursors, but reconciliation of the behaviour as revealed from different measurement techniques requires further work.

1015

Data availability



All the data used in this work can be accessed on the open database of the EUROCHAMP programme (<https://data.eurochamp.org/data-access/chamber-experiments/>).

Competing interests

1020 The authors declare that they have no conflict of interest.

Author contributions

GM, MRA, AV, YW and YS conceived the study. AV, YW, YS and MD conducted the experiments. YS conducted the data analysis and wrote the manuscript with contribution from all co-authors.

1025

Acknowledgements

The Manchester Aerosol Chamber acknowledges the funding support from the European Union's Horizon 2020 research and innovation programme under grant agreement no. 730997, which supports the EUROCHAMP2020 research programme. Instrumentational support was funded by the NERC Atmospheric Measurement and Observational Facility (AMOF). Y.W. acknowledges the joint scholarship of The University of Manchester and Chinese Scholarship Council. M.R.A. acknowledges funding support by UK National Centre for Atmospheric Sciences (NACS). A.V. acknowledges the funding support by Natural Environment Research Council (NERC) EAO Doctoral Training Partnership. The authors would also like to thank Kelly Pereira for on-site UHPLC-HRMS training for filter analysis and for providing the automated non-targeted analysis method for UHPLC-HRMS. I acknowledge the use of ChatGPT AI tool to proof-reading and correct grammar at the final stage of the writing process for this paper, which I reviewed, edited, and take full responsibility for. All final wording reflects my own edits and judgment.

1040



Reference

- Ahlberg, E., Falk, J., Eriksson, A., Holst, T., Brune, W. H., Kristensson, A., Roldin, P., and Svenningsson, B.: Secondary organic aerosol from VOC mixtures in an oxidation flow reactor, *Atmospheric Environment*, 161, 210-220, <https://doi.org/10.1016/j.atmosenv.2017.05.005>, 2017.
- Aiken, A. C., DeCarlo, P. F., Kroll, J. H., Worsnop, D. R., Huffman, J. A., Docherty, K. S., Ulbrich, I. M., Mohr, C., Kimmel, J. R., Sueper, D., Sun, Y., Zhang, Q., Trimborn, A., Northway, M., Ziemann, P. J., Canagaratna, M. R., Onasch, T. B., Alfarra, M. R., Prevot, A. S. H., Dommen, J., Duplissy, J., Metzger, A., Baltensperger, U., and Jimenez, J. L.: O/C and OM/OC Ratios of Primary, Secondary, and Ambient Organic Aerosols with High-Resolution Time-of-Flight Aerosol Mass Spectrometry, *Environmental Science & Technology*, 42, 4478-4485, [10.1021/es703009q](https://doi.org/10.1021/es703009q), 2008.
- Alfarra, M. R., Coe, H., Allan, J. D., Bower, K. N., Boudries, H., Canagaratna, M. R., Jimenez, J. L., Jayne, J. T., Garforth, A. A., Li, S.-M., and Worsnop, D. R.: Characterization of urban and rural organic particulate in the Lower Fraser Valley using two Aerodyne Aerosol Mass Spectrometers, *Atmospheric Environment*, 38, 5745-5758, <https://doi.org/10.1016/j.atmosenv.2004.01.054>, 2004.
- Atkinson, R. B., D. L. Cox, R. A. Crowley, J. N. Hampson, R. F. Hynes, R. G. Jenkin, M. E. Rossi, M. J. Troe, J.: Evaluated kinetic and photochemical data for atmospheric chemistry: Volume I - gas phase reactions of Ox, HOx, NOx and SOx species, *Atmos. Chem. Phys.*, 4, 1738, [10.5194/acp-4-1461-2004](https://doi.org/10.5194/acp-4-1461-2004), 2004.
- Bruns, E. A., Perraud, V., Zelenyuk, A., Ezell, M. J., Johnson, S. N., Yu, Y., Imre, D., Finlayson-Pitts, B. J., and Alexander, M. L.: Comparison of FTIR and Particle Mass Spectrometry for the Measurement of Particulate Organic Nitrates, *Environmental Science & Technology*, 44, 1056-1061, [10.1021/es9029864](https://doi.org/10.1021/es9029864), 2010.
- Carlton, A. G., Wiedinmyer, C., and Kroll, J. H.: A review of Secondary Organic Aerosol (SOA) formation from isoprene, *Atmos. Chem. Phys.*, 9, 4987-5005, [10.5194/acp-9-4987-2009](https://doi.org/10.5194/acp-9-4987-2009), 2009.
- Chhabra, P. S., Flagan, R. C., and Seinfeld, J. H.: Elemental analysis of chamber organic aerosol using an aerodyne high-resolution aerosol mass spectrometer, *Atmos. Chem. Phys.*, 10, 4111-4131, [10.5194/acp-10-4111-2010](https://doi.org/10.5194/acp-10-4111-2010), 2010.
- D. Sueper and collaborators, 2020. ToF-AMS Data Analysis Software Webpage, http://cires1.colorado.edu/jimenez-group/wiki/index.php/ToF-AMS_Analysis_Software
- D'Ambro, E. L., Schobesberger, S., Gaston, C. J., Lopez-Hilfiker, F. D., Lee, B. H., Liu, J., Zelenyuk, A., Bell, D., Cappa, C. D., Helgestad, T., Li, Z., Guenther, A., Wang, J., Wise, M., Caylor, R., Surratt, J. D., Riedel, T., Hyttinen, N., Salo, V. T., Hasan, G., Kurtén, T., Shilling, J. E., and Thornton, J. A.: Chamber-based insights into the factors controlling epoxydiol (IEPOX) secondary organic aerosol (SOA) yield, composition, and volatility, *Atmos. Chem. Phys.*, 19, 11253-11265, [10.5194/acp-19-11253-2019](https://doi.org/10.5194/acp-19-11253-2019), 2019.
- Daumit, K. E., Kessler, S. H., and Kroll, J. H.: Average chemical properties and potential formation pathways of highly oxidized organic aerosol, *Faraday Discuss*, 165, 181-202, [10.1039/c3fd00045a](https://doi.org/10.1039/c3fd00045a), 2013.
- DeCarlo, P. F., Kimmel, J. R., Trimborn, A., Northway, M. J., Jayne, J. T., Aiken, A. C., Gonin, M., Fuhrer, K., Horvath, T., Docherty, K. S., Worsnop, D. R., and Jimenez, J. L.: Field-Deployable,



- 1085 High-Resolution, Time-of-Flight Aerosol Mass Spectrometer, *Analytical Chemistry*, 78, 8281-8289, 10.1021/ac061249n, 2006.
- Docherty, K. S., Corse, E. W., Jaoui, M., Offenberg, J. H., Kleindienst, T. E., Krug, J. D., Riedel, T. P., and Lewandowski, M.: Trends in the oxidation and relative volatility of chamber-generated secondary organic aerosol, *Aerosol Science and Technology*, 52, 992-1004, 10.1080/02786826.2018.1500014, 2018.
- 1090 Du, M., Voliotis, A., Shao, Y., Wang, Y., Bannan, T. J., Pereira, K. L., Hamilton, J. F., Percival, C. J., Alfarra, M. R., and McFiggans, G.: Combined application of Online FIGAERO-CIMS and Offline LC-Orbitrap MS to Characterize the Chemical Composition of SOA in Smog Chamber Studies, *Atmos. Meas. Tech. Discuss.*, 2021, 1-42, 10.5194/amt-2021-420, 2021.
- 1095 Eddingsaas, N. C., Loza, C. L., Yee, L. D., Chan, M., Schilling, K. A., Chhabra, P. S., Seinfeld, J. H., and Wennberg, P. O.: α -pinene photooxidation under controlled chemical conditions – Part 2: SOA yield and composition in low- and high-NO_x environments, *Atmos. Chem. Phys.*, 12, 7413-7427, 10.5194/acp-12-7413-2012, 2012.
- Farmer, D. K., Matsunaga, A., Docherty, K. S., Surratt, J. D., Seinfeld, J. H., Ziemann, P. J., and Jimenez, J. L.: Response of an aerosol mass spectrometer to organonitrates and organosulfates and implications for atmospheric chemistry, *Proceedings of the National Academy of Sciences*, 107, 6670, 10.1073/pnas.0912340107, 2010.
- 1100 Fry, J. L., Kiendler-Scharr, A., Rollins, A. W., Wooldridge, P. J., Brown, S. S., Fuchs, H., Dubé, W., Mensah, A., dal Maso, M., Tillmann, R., Dorn, H. P., Brauers, T., and Cohen, R. C.: Organic nitrate and secondary organic aerosol yield from NO₃ oxidation of β -pinene evaluated using a gas-phase kinetics/aerosol partitioning model, *Atmos. Chem. Phys.*, 9, 1431-1449, 10.5194/acp-9-1431-2009, 2009.
- 1105 Henry, K. M., Lohaus, T., and Donahue, N. M.: Organic Aerosol Yields from α -Pinene Oxidation: Bridging the Gap between First-Generation Yields and Aging Chemistry, *Environmental Science & Technology*, 46, 12347-12354, 10.1021/es302060y, 2012.
- 1110 Hildebrandt, L., Henry, K. M., Kroll, J. H., Worsnop, D. R., Pandis, S. N., and Donahue, N. M.: Evaluating the Mixing of Organic Aerosol Components Using High-Resolution Aerosol Mass Spectrometry, *Environmental Science & Technology*, 45, 6329-6335, 10.1021/es200825g, 2011.
- Hoffmann, T., Huang, R.-J., and Kalberer, M.: Atmospheric Analytical Chemistry, *Analytical Chemistry*, 83, 4649-4664, 10.1021/ac2010718, 2011.
- 1115 Hoffmann, T., Odum, J. R., Bowman, F., Collins, D., Klockow, D., Flagan, R. C., and Seinfeld, J. H.: Formation of Organic Aerosols from the Oxidation of Biogenic Hydrocarbons, *Journal of Atmospheric Chemistry*, 26, 189-222, 10.1023/A:1005734301837, 1997.
- Jayne, J. T., Leard, D. C., Zhang, X., Davidovits, P., Smith, K. A., Kolb, C. E., and Worsnop, D. R.: Development of an aerosol mass spectrometer for size and composition analysis of submicron particles, *Aerosol Science & Technology*, 33, 49-70, 2000.
- 1120 Jimenez, J. L., Jayne, J. T., Shi, Q., Kolb, C. E., Worsnop, D. R., Yourshaw, I., Seinfeld, J. H., Flagan, R. C., Zhang, X., Smith, K. A., Morris, J. W., and Davidovits, P.: Ambient aerosol sampling using the Aerodyne Aerosol Mass Spectrometer, *Journal of Geophysical Research: Atmospheres*, 108, <https://doi.org/10.1029/2001JD001213>, 2003.
- 1125 Kroll, J. H., Lim, C. Y., Kessler, S. H., and Wilson, K. R.: Heterogeneous Oxidation of Atmospheric Organic Aerosol: Kinetics of Changes to the Amount and Oxidation State of Particle-Phase



- Organic Carbon, *The Journal of Physical Chemistry A*, **119**, 10767-10783, 10.1021/acs.jpca.5b06946, 2015.
- 1130 Kroll, J. H., Ng, N. L., Murphy, S. M., Flagan, R. C., and Seinfeld, J. H.: Secondary organic aerosol formation from isoprene photooxidation under high-NO_x conditions, *Geophysical Research Letters*, **32**, <https://doi.org/10.1029/2005GL023637>, 2005a.
- Kroll, J. H., Ng, N. L., Murphy, S. M., Varutbangkul, V., Flagan, R. C., and Seinfeld, J. H.: Chamber studies of secondary organic aerosol growth by reactive uptake of simple carbonyl compounds, *Journal of Geophysical Research: Atmospheres*, **110**, <https://doi.org/10.1029/2005JD006004>, 2005b.
- 1135 Kroll, J. H., Donahue, N. M., Jimenez, J. L., Kessler, S. H., Canagaratna, M. R., Wilson, K. R., Altieri, K. E., Mazzoleni, L. R., Wozniak, A. S., Bluhm, H., Mysak, E. R., Smith, J. D., Kolb, C. E., and Worsnop, D. R.: Carbon oxidation state as a metric for describing the chemistry of atmospheric organic aerosol, *Nature Chemistry*, **3**, 133-139, 10.1038/nchem.948, 2011.
- 1140 Lee, B.-H., Pierce, J. R., Engelhart, G. J., and Pandis, S. N.: Volatility of secondary organic aerosol from the ozonolysis of monoterpenes, *Atmospheric Environment*, **45**, 2443-2452, <https://doi.org/10.1016/j.atmosenv.2011.02.004>, 2011.
- Lee, B. H., Lopez-Hilfiker, F. D., Mohr, C., Kurtén, T., Worsnop, D. R., and Thornton, J. A.: An Iodide-Adduct High-Resolution Time-of-Flight Chemical-Ionization Mass Spectrometer: Application to Atmospheric Inorganic and Organic Compounds, *Environmental Science & Technology*, **48**, 6309-6317, 10.1021/es500362a, 2014.
- 1145 Li, K., Zhang, X., Zhao, B., Bloss, W. J., Lin, C., White, S., Yu, H., Chen, L., Geng, C., Yang, W., Azzi, M., George, C., and Bai, Z.: Suppression of anthropogenic secondary organic aerosol formation by isoprene, *npj Climate and Atmospheric Science*, **5**, 12, 10.1038/s41612-022-00233-x, 2022.
- 1150 Lopez-Hilfiker, F. D., Mohr, C., Ehn, M., Rubach, F., Kleist, E., Wildt, J., Mentel, T. F., Lutz, A., Hallquist, M., Worsnop, D., and Thornton, J. A.: A novel method for online analysis of gas and particle composition: description and evaluation of a Filter Inlet for Gases and AEROSols (FIGAERO), *Atmos. Meas. Tech.*, **7**, 983-1001, 10.5194/amt-7-983-2014, 2014.
- McFiggans, G., Mentel, T. F., Wildt, J., Pullinen, I., Kang, S., Kleist, E., Schmitt, S., Springer, M., 1155 Tillmann, R., and Wu, C.: Secondary organic aerosol reduced by mixture of atmospheric vapours, *Nature*, **565**, 587, 2019.
- Pandis, S. N., Paulson, S. E., Seinfeld, J. H., and Flagan, R. C.: Aerosol formation in the photooxidation of isoprene and β -pinene, *Atmospheric Environment. Part A. General Topics*, **25**, 997-1008, [https://doi.org/10.1016/0960-1686\(91\)90141-S](https://doi.org/10.1016/0960-1686(91)90141-S), 1991.
- 1160 Pereira, K., Ward, M., Wilkinson, J., Sallach, J., Bryant, D., Dixon, W., Hamilton, J., and Lewis, A.: An Automated Methodology for Non-targeted Compositional Analysis of Small Molecules in High Complexity Environmental Matrices Using Coupled Ultra Performance Liquid Chromatography Orbitrap Mass Spectrometry, *Environmental Science & Technology*, XXXX, 10.1021/acs.est.0c08208, 2021.
- 1165 Presto, A. A., Miracolo, M. A., Kroll, J. H., Worsnop, D. R., Robinson, A. L., and Donahue, N. M.: Intermediate-Volatility Organic Compounds: A Potential Source of Ambient Oxidized Organic Aerosol, *Environmental Science & Technology*, **43**, 4744-4749, 10.1021/es803219q, 2009.
- Pullinen, I., Schmitt, S., Kang, S., Sarrafzadeh, M., Schlag, P., Andres, S., Kleist, E., Mentel, T. F., Rohrer, F., Springer, M., Tillmann, R., Wildt, J., Wu, C., Zhao, D., Wahner, A., and Kiendler-Scharr, A.: Impact of NO_x on secondary organic aerosol (SOA) formation from α -pinene and β -
- 1170



- pinene photooxidation: the role of highly oxygenated organic nitrates, *Atmos. Chem. Phys.*, **20**, 10125-10147, 10.5194/acp-20-10125-2020, 2020.
- 1175 Shao, Y., Voliotis, A., Du, M., Wang, Y., Pereira, K., Hamilton, J., Alfarra, M. R., and McFiggans, G.: Chemical composition of secondary organic aerosol particles formed from mixtures of anthropogenic and biogenic precursors, *Atmos. Chem. Phys.*, **22**, 9799-9826, 10.5194/acp-22-9799-2022, 2022a.
- Shao, Y., Wang, Y., Du, M., Voliotis, A., Alfarra, M. R., O'Meara, S. P., Turner, S. F., and McFiggans, G.: Characterisation of the Manchester Aerosol Chamber facility, *Atmos. Meas. Tech.*, **15**, 539-559, 10.5194/amt-15-539-2022, 2022b.
- 1180 Shilling, J. E., Chen, Q., King, S. M., Rosenoern, T., Kroll, J. H., Worsnop, D. R., DeCarlo, P. F., Aiken, A. C., Sueper, D., Jimenez, J. L., and Martin, S. T.: Loading-dependent elemental composition of α -pinene SOA particles, *Atmos. Chem. Phys.*, **9**, 771-782, 10.5194/acp-9-771-2009, 2009.
- 1185 Stark, H., Yatavelli, R. L. N., Thompson, S. L., Kimmel, J. R., Cubison, M. J., Chhabra, P. S., Canagaratna, M. R., Jayne, J. T., Worsnop, D. R., and Jimenez, J. L.: Methods to extract molecular and bulk chemical information from series of complex mass spectra with limited mass resolution, *International Journal of Mass Spectrometry*, **389**, 26-38, <https://doi.org/10.1016/j.ijms.2015.08.011>, 2015.
- 1190 Stroud, C. A., Roberts, J. M., Goldan, P. D., Kuster, W. C., Murphy, P. C., Williams, E. J., Hereid, D., Parrish, D., Sueper, D., Trainer, M., Fehsenfeld, F. C., Apel, E. C., Riemer, D., Wert, B., Henry, B., Fried, A., Martinez-Harder, M., Harder, H., Brune, W. H., Li, G., Xie, H., and Young, V. L.: Isoprene and its oxidation products, methacrolein and methylvinyl ketone, at an urban forested site during the 1999 Southern Oxidants Study, *Journal of Geophysical Research: Atmospheres*, **106**, 8035-8046, <https://doi.org/10.1029/2000JD900628>, 2001.
- 1195 Surratt, J. D., Kroll, J. H., Kleindienst, T. E., Edney, E. O., Claeys, M., Sorooshian, A., Ng, N. L., Offenberg, J. H., Lewandowski, M., Jaoui, M., Flagan, R. C., and Seinfeld, J. H.: Evidence for Organosulfates in Secondary Organic Aerosol, *Environmental Science & Technology*, **41**, 517-527, 10.1021/es062081q, 2007.
- 1200 Surratt, J. D., Gómez-González, Y., Chan, A. W. H., Vermeylen, R., Shahgholi, M., Kleindienst, T. E., Edney, E. O., Offenberg, J. H., Lewandowski, M., Jaoui, M., Maenhaut, W., Claeys, M., Flagan, R. C., and Seinfeld, J. H.: Organosulfate Formation in Biogenic Secondary Organic Aerosol, *The Journal of Physical Chemistry A*, **112**, 8345-8378, 10.1021/jp802310p, 2008.
- 1205 Voliotis, A., Wang, Y., Shao, Y., Du, M., Bannan, T. J., Percival, C. J., Pandis, S. N., Alfarra, M. R., and McFiggans, G.: Exploring the composition and volatility of secondary organic aerosols in mixed anthropogenic and biogenic precursor systems, *Atmos. Chem. Phys. Discuss.*, **2021**, 1-39, 10.5194/acp-2021-215, 2021.
- 1210 Voliotis, A., Du, M., Wang, Y., Shao, Y., Bannan, T. J., Flynn, M., Pandis, S. N., Percival, C. J., Alfarra, M. R., and McFiggans, G.: The influence of the addition of isoprene on the volatility of particles formed from the photo-oxidation of anthropogenic-biogenic mixtures, *Atmos. Chem. Phys.*, **22**, 13677-13693, 10.5194/acp-22-13677-2022, 2022a.
- Voliotis, A., Du, M., Wang, Y., Shao, Y., Alfarra, M. R., Bannan, T. J., Hu, D., Pereira, K. L., Hamilton, J. F., Hallquist, M., Mentel, T. F., and McFiggans, G.: Chamber investigation of the formation and transformation of secondary organic aerosol in mixtures of biogenic and



- 1215 anthropogenic volatile organic compounds, *Atmos. Chem. Phys. Discuss.*, 2022, 1-49,
10.5194/acp-2021-1080, 2022b.
Wennberg, P. O., Bates, K. H., Crouse, J. D., Dodson, L. G., McVay, R. C., Mertens, L. A.,
Nguyen, T. B., Praske, E., Schwantes, R. H., Smarte, M. D., St Clair, J. M., Teng, A. P., Zhang, X.,
and Seinfeld, J. H.: Gas-Phase Reactions of Isoprene and Its Major Oxidation Products, *Chemical
Reviews*, 118, 3337-3390, 10.1021/acs.chemrev.7b00439, 2018.
- 1220 Winterhalter, R., Van Dingenen, R., Larsen, B. R., Jensen, N. R., and Hjorth, J.: LC-MS analysis of
aerosol particles from the oxidation of α -pinene by ozone and OH-radicals, *Atmos. Chem.
Phys. Discuss.*, 2003, 1-39, 10.5194/acpd-3-1-2003, 2003.
Xu, L., Middlebrook, A. M., Liao, J., de Gouw, J. A., Guo, H., Weber, R. J., Nenes, A., Lopez-
Hilfiker, F. D., Lee, B. H., Thornton, J. A., Brock, C. A., Neuman, J. A., Nowak, J. B., Pollack, I. B.,
1225 Welti, A., Graus, M., Warneke, C., and Ng, N. L.: Enhanced formation of isoprene-derived
organic aerosol in sulfur-rich power plant plumes during Southeast Nexus, *Journal of
Geophysical Research: Atmospheres*, 121, 11,137-111,153, 10.1002/2016jd025156, 2016.
Zhao, Y., Zhao, Y., Wang, C., Shao, Y., Xie, H., Yang, J., Zhang, W., Wu, G., Li, G., Jiang, L., and
Yang, X.: Photooxidation and ozonolysis of α -pinene and limonene mixtures: Mechanisms of
1230 secondary organic aerosol formation and cross-dimerization, *Journal of Environmental
Sciences*, <https://doi.org/10.1016/j.jes.2025.04.020>, 2025.
Zhao, Y., Zhao, Y., Wang, C., Shao, Y., Xie, H., Yang, J., Zhang, W., Wu, G., Li, G., Jiang, L., and
Yang, X.: Photooxidation and ozonolysis of α -pinene and limonene mixtures: Mechanisms of
secondary organic aerosol formation and cross-dimerization, *Journal of Environmental
1235 Sciences*, <https://doi.org/10.1016/j.jes.2025.04.020>, 2025.

1240